Commun. Math. Phys. 138, 63–105 (1991)

Communications in
Mathematical
Physics

Graph Theory, $SO(n)$ Current Algebra and the Virasoro Master Equation*

M. B. Halpern and N. A. Obers

Department of Physics, University of California, and Theoretical Physics Group,
Physics Division, Lawrence Berkeley Laboratory, 1 Cyclotron Road, Berkeley, CA 94720, USA

Received August 1, 1990

Abstract. We announce an isomorphism between a set of generically irrational affine-Virasoro constructions on $SO(n)$ and the unlabelled graphs of order n. On the one hand, the conformal constructions are classified by the graphs, while, conversely, a group-theoretic and conformal field-theoretic identification is obtained for every graph of graph theory. High-level expansion provides a strong argument that each construction is unitary down to some finite critical level.

Table of Contents

* This work was supported in part by the Director, Office of Energy Research, Office of High Energy and Nuclear Physics, Division of High Energy Physics of the U.S. Department of Energy under Contract DE-AC03-76SF00098 and in part by the National Science Foundation under grant PHY85-15857

1. Introduction

Affine Lie algebra, or current algebra on S_1, was discovered independently in mathematics [1] and physics [2]. The first representations [2] were constructed with world-sheet fermions [2, 3] to implement the proposal of current-algebraic spin and internal symmetry on the string [2]. Examples of affine-Sugawara constructions [2, 4] and coset constructions [2, 4] were also given in the first string era, as well as the vertex operator construction of fermions and $SU(n)_1$ from compactified spatial dimensions [5, 6]. The generalization of these constructions [7–9] and their applications to the heterotic string [10] mark the beginning of the present era. See [11–14] for further historical remarks on affine-Virasoro constructions.

The general Virasoro construction on affine g [15–17]

$$T(L) = L^{ab} {}^{*}_{*} J_a J_b {}^{*}_{*} \tag{1.1}$$

systematizes the direct approach used by Bardakdi and Halpern [2, 4] to obtain the original affine-Sugawara and coset constructions. The resulting Virasoro master equation [15–17] for the inverse inertia tensor $L^{ab} = L^{ba}$ contains the affine-Sugawara nests[1] and many new conformal constructions $g^{\#}$ on the currents of affine g.

In particular, broad classes of exact solutions with unitary irrational central charge on compact g have recently been announced [18]. The growing list presently includes the unitary irrational constructions [18, 20–22]

$$((\text{simply-laced } g_x)^q)^{\#}_M$$

$$SU(3)^{\#}_{\text{BASIC}} = \begin{cases} SU(3)^{\#}_M \\ SU(3)^{\#}_{D(1)}, SU(3)^{\#}_{D(2)}, SU(3)^{\#}_{D(3)} \\ SU(3)^{\#}_{A(1)}, SU(3)^{\#}_{A(2)} \end{cases} \tag{1.2}$$

[1] The affine-Sugawara nests [18] include the affine-Sugawara constructions [2, 4, 8], the coset constructions [2, 4, 9] and the nested coset constructions [19]

which are obtained in the BASIC$\supset$Dynkin$\supset$Maximal sequence of subansätze, ordered according to increasing discrete symmetry. The value

$$c((SU(3)_5)^{\#}_{D(1)})=2\left(1-\frac{1}{\sqrt{61}}\right)\simeq 1.7439 \tag{1.3}$$

is the lowest unitary irrational central charge yet observed [22].

A very large number [18]

$$N(g)=2^{n(g)}, \qquad n(g)=\dim g(\dim g-1)/2 \tag{1.4}$$

of solutions is expected generically on arbitrary level of any g, e.g. $N(g)\approx\frac{1}{4}$ billion on $SU(3)$, so the exact constructions in Eq. (1.2) are only the first glimpse into a generically-irrational affine-Virasoro universe of immense new structure.

A high-level (semi-classical) expansion of the master equation [22] has been developed which marks a bifurcation in the study of new conformal constructions on affine g: In one direction, the expansion is capable in principle of seeing all solutions whose high-level behavior is $\mathcal{O}(k^{-1})$, which includes all high-k smooth unitary solutions [18]. Following [23], we refer to these $\mathcal{O}(k^{-1})$ constructions as the class of *high-k smooth* constructions on g. In another direction, the classical limit of the master equation is a cornerstone of the generic affine-Virasoro action [23], which begins the irrational conformal field theory of the generic high-k smooth construction.

The purpose of this paper is the detailed study, primarily by high-level expansion, of a new ansatz

$$SO(n)_{\text{diag}}: \quad \text{the diagonal ansatz on } SO(n)$$

whose set of high-k smooth constructions is generically irrational. High-level analysis provides a strong argument that each of these constructions is unitary down to some finite critical level, in accord with our experience in [18, 20–22] and the additional exact solutions of this paper.

Our central result is that the physically distinct [20, 22] high-k smooth constructions in $SO(n)_{\text{diag}}$ are in one-to-one correspondence with the unlabelled graphs of graph theory [24, 25]:

$$\begin{aligned}&\text{each distinct (high-}k\text{ smooth) affine-Virasoro construction in } SO(n)_{\text{diag}}\\ &\qquad\leftrightarrow \text{each unlabelled graph of order } n.\end{aligned} \tag{1.5}$$

This means, on the one hand, that the high-k smooth constructions in $SO(n)_{\text{diag}}$ are classified by the set of all graphs. Conversely, a group-theoretic and conformal field-theoretic identification is obtained for every graph of graph theory, which may be interesting in mathematics.

The isomorphism begins a cross-fertilization of the subjects:

1. Graph theory $\to$ conformal field theory

Beyond taxonomy, graph theory is important in counting constructions and the analysis of residual automorphisms [20, 22], symmetries, consistent subansätze and exact solutions.

For example, the asymptotic results

$$N(SO(n))=\mathcal{O}(e^{n^4(\ln 2)/8}), \tag{1.6a}$$

$$N(SO(n)_{\text{diag}}=\text{graphs of order } n)=\mathcal{O}(e^{n^2(\ln 2)/2}), \tag{1.6b}$$

$$N(\text{affine-Sugawara nests in } SO(n)_{\text{diag}})\leqq\mathcal{O}(e^{2n\ln 2}) \tag{1.6c}$$

are seen at large n for the total number of constructions on $SO(n)$, the number of unlabelled graphs, and the number of affine-Sugawara nests in $SO(n)_{\mathrm{diag}}$. The asymptotic forms (1.6b, c) show a dramatic dominance of new constructions over old constructions, so that

$$\text{the generic graph in } SO(n \gg 1)_{\mathrm{diag}} \text{ is a new construction}. \tag{1.7}$$

It also follows from (1.6a, b) that the full space of solutions on $SO(n)$ is a structure which is much larger than graph theory.

Graph theory was particularly helpful in finding the new *self-K-conjugate constructions*, which are the self-complementary graphs [24] of graph theory. These constructions live only on $SO(4n)$ and $SO(4n+1)$ with *half-Sugawara central charge*, whose values raise the question of new rational central charges.

Graph symmetry also determines a hierarchy of consistent subansätze in $SO(n)_{\mathrm{diag}}$. Beginning with the smallest subansätze, we report the following exact unitary irrational constructions,

$$\begin{gathered} SO(2n)^{\#}[d,4]\,, \quad n \geqq 3 \\ SO(2n+1)^{\#}[d,6]_1\,, \quad n \geqq 3 \\ SO(2n+1)^{\#}[d,6]_2\,, \quad n \geqq 3 \\ SO(5)^{\#}[d,6]_2\,. \end{gathered} \tag{1.8}$$

The names of these constructions include the size of the smallest subansatz in which their graphs appear, and we remark that the constructions on $SO(2n+1)$ are the first unitary irrational constructions on non-simply-laced g. The maximal-symmetric construction $SO(2n)_M^{\#}$ [18] also occurs as the most symmetric set of graphs in $SO(2n)_{\mathrm{diag}}^{\#}$.

2. Conformal field theory $\rightarrow$ graph theory

Translating from conformal field theory, we find a number of equivalent categories in graph theory,

- affine-Sugawara construction = complete graph
- K-conjugate construction = complement of a graph
- coset construction = complete N-partite graph

and a number of categories which are apparently new in graph theory,

- the affine-Sugawara nested graphs
- the graphs $G_n^{\#}$ of the new constructions $SO(n)_{\mathrm{diag}}^{\#}$
- the affine-Virasoro nested graphs
- the irreducible and new irreducible graphs
- the broken $N=2$ affine-Sugawara nested graphs.

In general, the names of these graphs are derived from their corresponding conformal constructions. The irreducible graphs are particularly important because every graph can be uniquely constructed from the irreducible graphs by affine-Virasoro nesting [18].

We have also constructed a graph function $\nu(G)$, the novelty number of G, which appears to act as an order parameter for the graphs $G^{\#}$ of new constructions.

2. General Virasoro Construction on Affine g

2.1. The Virasoro Master Equation. The general affine-Virasoro construction is [15, 17]

$$T(L) \equiv L^{ab} {}^*_* J_a J_b {}^*_*, \; [L^{(m)}, L^{(n)}] = (m-n) L^{(m+n)} + \frac{c}{12} m(m^2-1)\delta_{m+n,0} \tag{2.1}$$

with symmetric normal ordering $T_{ab} = {}^*_* J_a J_b {}^*_* = T_{ba}$ [15] on the currents J_a of affine g [1, 2]

$$[J_a^{(m)}, J_b^{(n)}] = i f_{ab}^c J_c^{(m+n)} + m G_{ab} \delta_{m+n,0}, \tag{2.2}$$

where f_{ab}^c and G_{ab} are respectively the structure constants and general Killing metric of g. Analysis of the system (2.1–2) results in the Virasoro master equation and central charge [15, 17]

$$\begin{gathered} L^{ab} = 2L^{ac} G_{cd} L^{db} - L^{cd} L^{ef} f_{ce}^a f_{df}^b - L^{cd} f_{ce}^f f_{df}^{(a} L^{b)e}, \\ c = 2G_{ab} L^{ab} \end{gathered} \tag{2.3}$$

for the inverse inertia tensor $L^{ab} = L^{ba}$ of the Virasoro operator (2.1). The construction is completely general since g is not necessarily compact or semisimple. In particular, to obtain level $x_I = 2k_I/\psi_I^2$ of g_I in $g = \oplus_I g_I$ with dual Coxeter number $\tilde{h}_I = Q_I/\psi_I^2$, take

$$G_{ab} = \oplus_I k_I \eta_{ab}^I, \qquad f_{ac}^d f_{bd}^c = -\oplus_I Q_I \eta_{ab}^I, \tag{2.4}$$

where η_{ab}^I is a Killing metric of g_I. The master equation has been identified in [16] as an Einstein-like system on the group manifold: The central charge of the general construction is $c = \dim g - 4R$, where R is the curvature scalar.

We remark on some general properties of the master equation which will be useful in the analysis below:

1. The affine-Sugawara construction [2, 4, 8] L_g is

$$L_g^{ab} = \oplus_I \frac{\eta_I^{ab}}{2k_I + Q_I}, \qquad c_g = \sum_I \frac{x_I \dim g_I}{x_I + \tilde{h}_I} \tag{2.5}$$

for arbitrary level of any g, and similarly for L_h when $h \subset g$.

2. K-conjugation covariance [2, 4, 9, 15]. When L is a solution of the master equation on g, then so is the K-conjugate partner $\tilde{L}$ of L,

$$\tilde{L}^{ab} = L_g^{ab} - L^{ab}, \qquad \tilde{c} = c_g - c, \tag{2.6}$$

while the corresponding constructions $T(L)$ and $T(\tilde{L})$ form a commuting pair of Virasoro operators.

3. Affine-Virasoro nests [18]. Repeated embedding by K-conjugation produces the affine-Virasoro nests. For example, the nests on $g \supset h' \supset h$ are

$$\begin{gathered} L_h \text{ or } L_h^{\#} : (h \text{ or } h^{\#}), \\ L_{h'} - (L_h \text{ or } L_h^{\#}) : h'/(h \text{ or } h^{\#}), \\ L_g - L_{h'} + (L_h \text{ or } L_h^{\#}) : g/h'/(h \text{ or } h^{\#}), \end{gathered} \tag{2.7}$$

where L_h is the affine-Sugawara construction on h and $L_h^\#$ is any new construction $h^\#$ on h. According to Eq. (2.6), the central charges of these nests are (c_h or $c_h^\#$), $c_{h'}-(c_h$ or $c_h^\#)$ and $c_g-c_{h'}+(c_h$ or $c_h^\#)$ respectively. The special case of affine-Sugawara nests is realized by restriction to affine-Sugawara constructions at the bottom of the nests. Irreducible constructions [18] are reviewed in Sect. 2.2.

4. Counting. The master equation (2.3) is a system of $\dim g(\dim g+1)/2$ coupled quadratic equations on an equal number of unknowns $L^{ab}=L^{ba}$, so that a very large number [18]

$$N(g)=2^{n(g)}\,, \qquad n(g)=\dim g(\dim g-1)/2 \tag{2.8}$$

of solutions is expected generically on arbitrary level of affine g, after gauge fixing [22] the inner automorphisms of g. As in general relativity, new solutions of the master equation have generally been obtained with hierarchies of consistent ansätze and subansätze [18, 20, 22], beginning with the basic ansatz on simply-laced g [18].

5. Radial and angular variables. Unitarity on positive integer level of compact affine g requires [9, 18]

$$L^{ab}=\text{real} \tag{2.9}$$

in any Cartesian basis, so all unitary solutions are naturally included in the eigenbasis [22]

$$L^{ab}=\sum_c \Omega^{ac}\Omega^{bc}\lambda_c \tag{2.10}$$

with $\lambda_a=$ real the radial variables and $\Omega\in SO(\dim g)$ the angular variables. This eigenbasis is convenient for level x of simple compact g with

$$G_{ab}=k\delta_{ab}\,, \qquad x=2k/\psi^2\,, \tag{2.11}$$

since the master equation takes the form

$$\lambda_a(1-2k\lambda_a)=\sum_{cd}\lambda_c(2\lambda_a-\lambda_d)\hat{f}_{cda}^2\,, \tag{2.12a}$$

$$0=\sum_{cd}\lambda_c(\lambda_a+\lambda_b-\lambda_d)\hat{f}_{cda}\hat{f}_{cdb}\,, \qquad a<b\,, \tag{2.12b}$$

$$\hat{f}_{abc}\equiv f_{a'b'c'}\Omega^{a'a}\Omega^{b'b}\Omega^{c'c}\,, \tag{2.12c}$$

$$c=2k\sum_a \lambda_a \tag{2.12d}$$

with all Ω dependence in the $SO(\dim g)$-twisted structure constants $\hat{f}_{abc}$ of g.

6. High-level expansion. A high-level (semi-classical) expansion of the system (2.12) was developed in [22], which is capable in principle of seeing all high-k smooth ($\mathcal{O}(k^{-1})$) solutions of the master equation on any manifold. The results at leading order are [22]

$$L^{ab}\simeq\frac{1}{k}L^{ab}_{(0)}=\frac{1}{k}\sum_c \Omega^{ac}_{(0)}\Omega^{bc}_{(0)}\lambda_c^{(0)}\,, \qquad c\simeq c_0=\sum_a \theta_a\,, \tag{2.13a}$$

$$\lambda_a^{(0)}=\frac{\theta_a}{2}\,, \qquad \theta_a=0 \text{ or } 1\,, \qquad a=1,\ldots,\dim g\,, \tag{2.13b}$$

$$0=\sum_{cd}\theta_c(\theta_a+\theta_b-\theta_d)\hat{f}^{(0)}_{cda}\hat{f}^{(0)}_{cdb}\,, \qquad a<b\,, \tag{2.13c}$$

$$\hat{f}^{(0)}_{abc}=f_{a'b'c'}\Omega^{a'a}_{(0)}\Omega^{b'b}_{(0)}\Omega^{c'c}_{(0)}\,, \tag{2.13d}$$

so that, in particular, all high-k smooth constructions approach integer central charges c_0 at high level. Values of the high-k twist $\Omega_{(0)}$ are determined by the quantization condition (2.13c) (or higher-order analogues) for each choice $\{\theta_a\}$ of the radial variables. The high-level expansion was applied to see all the high-k smooth solutions on $SU(3)$ in the basic ansatz, and the expansion also provided structural clues which were sufficient to obtain the exact form of all the high-k smooth unitary irrational constructions $SU(3)^{\#}_{\mathrm{BASIC}}$ in the ansatz [22, 21].

The high-level expansion was simple for $SU(3)_{\mathrm{BASIC}}$ because the angular variable in this case [22],

$$\Omega^{ab}=\begin{pmatrix}\Omega^{AB}(\phi) & 0\\ 0 & 1\end{pmatrix},\qquad \Omega^{AB}(\phi)=\begin{pmatrix}\cos\phi & -\sin\phi\\ \sin\phi & \cos\phi\end{pmatrix} \tag{2.14}$$

is a single angle of rotation ϕ on the Cartan subalgebra, so that the quantization condition (2.13c) is a one dimensional problem. More generally, the quantization condition (2.13c) on the angular variables will be progressively more difficult to solve on larger groups.

One hope for simplification of the master equation and its high-level expansion is the existence of small consistent ansätze, such as the metric ansatz

$$L^{ab}=\tfrac{1}{2}(\lambda_a+\lambda_b)\eta^{ab}, \tag{2.15}$$

where η_{ab} is the Killing metric on compact g. The consistency of a metric ansatz is generally basis dependent, since the form (2.15) is not covariant. We restrict our discussion here to the case of Cartesian coordinates, where the metric ansatz becomes a *diagonal ansatz*

$$L^{ab}=\lambda_a\delta_{ab}, \tag{2.16a}$$

$$\lambda_a(1-2k\lambda_a)=\sum_{cd}\lambda_c(2\lambda_a-\lambda_d)f_{cda}^2, \tag{2.16b}$$

$$f_{cd}^{a}f_{cd}^{b>a}=0,\qquad \forall c,d, \tag{2.16c}$$

$$c=2k\sum_a\lambda_a, \tag{2.16d}$$

whose consistency condition (2.16c) guarantees that the off-diagonal master equation (2.12b) is satisfied identically for $\Omega^{ab}=\delta^{ab}$. The consistency condition means that any two generators of g commute to no more than a single generator, which is not true for $SU(3)$ in, say, the Gell-Mann basis. As we note in the following section, however, the consistency condition is satisfied in the physicist's standard Cartesian basis for $SO(n)$. Metric ansätze on other manifolds are under investigation.

2.2. The Diagonal Ansatz on SO(n). We label the Cartesian generators J_{ij} of $SO(n\geqq 3)$ by the *vector indices* $1\leqq i<j\leqq n$, so that $a\equiv(i,j)=1,\dots,\dim g=n(n-1)/2$. The Cartesian structure constants and Killing metric are

$$f_{ij;kl}^{rs}\equiv\sqrt{\frac{\tau\psi^2}{2}}\,(\delta_{jk}\delta_i^{[r}\delta_l^{s]}-\delta_{jl}\delta_i^{[r}\delta_k^{s]}-\delta_{ik}\delta_j^{[r}\delta_l^{s]}+\delta_{il}\delta_j^{[r}\delta_k^{s]}) \tag{2.17a}$$

$$\eta_{ij;kl}\equiv\delta_{ik}\delta_{jl},\qquad \tau\equiv\begin{cases}2, & n=3\\ 1, & n\geqq 4\end{cases}, \tag{2.17b}$$

where ψ is the highest root of $SO(n)$ and $A^{[r}B^{s]} \equiv A^rB^s - A^sB^r$. The structure constants in this basis satisfy the consistency condition (2.16c) in the form

$$f_{ij;kl}^{rs} f_{ij;kl}^{tu \neq rs} = 0, \quad \forall (i,j) \text{ and } (k,l) \tag{2.18}$$

because (r,s) is uniquely determined for each fixed choice (i,j) and (k,l) when $f_{ij;kl}^{rs}$ is nonvanishing.

It follows that the diagonal ansatz on $SO(n)$,

$$SO(n)_{\text{diag}}: L^{ij;kl} \equiv \frac{L_{ij}}{\psi^2} \delta_{ik}\delta_{jl}, \quad T(L) = \frac{1}{\psi^2} \sum_{i<j} L_{ij} {}^*_*(J_{ij})^2{}^*_*, \tag{2.19}$$

is a consistent ansatz. The radial variables are $\lambda_{ij} = L_{ij}/\psi^2$, and the simplest form of the ansatz is obtained with the symmetrization convention

$$L_{ij} \equiv L_{ji}, \quad i \neq j; \quad L_{ii} \equiv 0. \tag{2.20}$$

The master equation for $SO(n)_{\text{diag}}$,

$$\begin{gathered} L_{ij}(1 - xL_{ij}) - \tau L_{ij} \sum_{l \neq i,j}^{n} (L_{il} + L_{jl}) + \tau \sum_{l \neq i,j}^{n} L_{il}L_{lj} = 0, \quad i<j, \\ c = x \sum_{i<j} L_{ij}, \end{gathered} \tag{2.21}$$

follows with Eqs. (2.17) and (2.19–20) from the radial equation (2.16).

The following properties of $SO(n)_{\text{diag}}$ will be useful below:

1. Counting. The master equation (2.21) in the diagonal ansatz shows $\dim SO(n) = \binom{n}{2}$ quadratic equations on an equal number of unknowns, so that

$$N(SO(n)_{\text{diag}}) = 2^{\binom{n}{2}} \tag{2.22}$$

solutions are expected generically for any level of $SO(n)_{\text{diag}}$.

2. Unitarity. Unitary solutions on positive integer level of $SO(n)_{\text{diag}}$ are recognized when

$$L_{ij} = \text{real}, \tag{2.23}$$

since the Cartesian currents satisfy $J_{ij}^{(m)\dagger} = J_{ij}^{(-m)}$.

3. K-conjugation covariance. According to Eq. (2.6), the K-conjugate construction $\tilde{L}_{ij}$,

$$\begin{gathered} \tilde{L}_{ij} = L_{ij}(SO(n)) - L_{ij}, \quad \tilde{c} = \frac{xn(n-1)/2}{x + \tau(n-2)} - c, \\ L_{ij}(SO(n)) = \frac{1}{x + \tau(n-2)} \end{gathered} \tag{2.24}$$

is obtained when L_{ij} is a construction in $SO(n)_{\text{diag}}$.

4. Subgroups, cosets and affine-Sugawara nests. The diagonal ansatz on $SO(n)$ contains only those subgroups

$$\begin{gathered} h(SO(n)_{\text{diag}}) \equiv SO(m_1) \times SO(m_2) \times \ldots \times SO(m_N) \\ \sum_{i=1}^{N} m_i = n, \quad 2 \leqq N \leqq n-1, \quad m_i \geqq 1 \end{gathered} \tag{2.25}$$

whose generators are a *subset* of the generators J_{ij} of $SO(n)$, and not linear combinations of these generators. Any $SO(1)$ factor in (2.25) is the trivial construction $L(SO(1))=0$. Moreover, each factor $SO(m_i)$ occurs in its own diagonal subansatz, $SO(m_i)_{\text{diag}}$, so further subgroup nesting follows the same pattern [2] within each $SO(m_i)$. Note that any factor $SO(3)$ is embedded at level $\tau x=2x$ in $SO(n\geqq 4)_x$, while $SO(m_i\geqq 4)$ is always a regular embedding.

We define the *fundamental* affine-Sugawara nests $\mathcal{N}_n$ in $SO(n)_{\text{diag}}$ as those obtained by subgroup nesting with $SO(n)$ at the top. Moreover, we will say that a fundamental nest $\mathcal{N}_n(d)$ has *depth d* when it contains d layers of subgroup nesting. The first three depths are

$$
\begin{aligned}
&d=1: SO(n),\\
&d=2: \frac{SO(n)}{h(SO(n)_{\text{diag}})},\\
&d=3: \frac{SO(n)}{\dfrac{SO(m_1)}{h(SO(m_1)_{\text{diag}})}\times SO(m_2)\times\ldots\times SO(m_N)}\\
&\qquad\;\; \frac{SO(n)}{\dfrac{SO(m_1)}{h(SO(m_1)_{\text{diag}})}\times\dfrac{SO(m_2)}{h(SO(m_2)_{\text{diag}})}\times\ldots\times SO(m_N)}\\
&\qquad\qquad \vdots\\
&\qquad\;\; \frac{SO(n)}{\dfrac{SO(m_1)}{h(SO(m_1)_{\text{diag}})}\times\dfrac{SO(m_2)}{h(SO(m_2)_{\text{diag}})}\times\ldots\times\dfrac{SO(m_N)}{h(SO(m_N)_{\text{diag}})}},
\end{aligned}
\tag{2.26}
$$

and so on for deeper nests. The *bottom* of each nest is the collection of constructions at the bottom of all the nesting columns. The fundamental affine-Sugawara nests $\mathcal{N}_n(d)$ and their K-conjugate nests $\tilde{\mathcal{N}}_n(d)$ on $SO(n)$ [3] form the set of all affine-Sugawara nests in $SO(n)_{\text{diag}}$, which are all known rational constructions in the ansatz.

5. Affine-Virasoro nests [18]. The more general fundamental affine-Virasoro nests on g are those constructed with g at the top, allowing general constructions on smaller manifolds at the bottom of each nest, including new constructions $h^\#$, $h\subset g$. Together, the fundamental affine-Virasoro nests and their K-conjugate nests form the set of all affine-Virasoro nests, which contains all affine-Virasoro constructions on g. Examples of fundamental affine-Virasoro nests in $SO(n)_{\text{diag}}$ include

$$
\frac{SO(n)}{SO(m<n)^\#},\quad \frac{SO(n)}{SO(m)^\#\times SO(n-m)},\quad \frac{SO(n)}{\dfrac{SO(m<n)}{SO(p<m)^\#}}
\tag{2.27}
$$

and the fundamental affine-Sugawara nests in Eq. (2.26).

---

[2] For example, $SO(2n)/(SO(n)\times SO(n))/SO(n)_V$, with $SO(n)_V$ the diagonal subgroup of $SO(n)\times SO(n)$, is excluded because this nest requires linear combinations of the generators J_{ij}

[3] The K-conjugate nests of the fundamental affine-Sugawara nests in Eq. (2.26) are obtained by removing $SO(n)$ from the top of each construction. More generally, the K-conjugate nests $\tilde{\mathcal{N}}_n(d)$ on $SO(n)$ are products of fundamental affine-Sugawara nests on smaller manifolds

6. Irreducible constructions [18]. The reducible constructions on g are the fundamental affine-Virasoro nests of depth $d \geqq 2$ and their K-conjugates on g, all of which involve subconstructions on smaller manifolds. The *irreducible constructions* on g are therefore the affine-Sugawara construction on g and any *new irreducible constructions* $g^{\#}$, $g/g^{\#}$ which contain no subconstructions on smaller manifolds. Note that the new irreducible constructions are such that *both* $g^{\#}$ and $g/g^{\#}$ are non-trivial irreducible constructions, whereas, the single "old" irreducible affine-Sugawara construction is K-conjugate to the trivial construction $L=0$ on g. The maximal-symmetric constructions [18]

$$SO(2n)^{\#}_{M}, \qquad SO(2n)/SO(2n)^{\#}_{M} \tag{2.28}$$

are examples of known irreducible constructions which are also found in $SO(2n)_{\text{diag}}$.

Irreducible constructions are important because affine-Virasoro space may be organized as the set of fundamental affine-Virasoro nests with irreducible constructions at the bottom of each nest, plus the K-conjugates of these constructions. Moreover, since all irreducible constructions nest identically into larger groups, the irreducible constructions provide a fundamental measure of old versus new constructions, which, loosely speaking, mods out by the affine-Virasoro nesting.

7. $SO(n)$ automorphisms and vector-index relabelling. After gauge-fixing the master equation (or its consistent ansätze), there generally remains a discrete set of residual level-independent automorphisms [20, 22] under which the master equation transforms covariantly. The residual automorphisms divide the solutions L into *physically equivalent* sets of solutions called automorphism cycles whose members have the same central charge and conformal weights. We refer below to the automorphism class of any solution L as auto L.

In the case of $SO(n)_{\text{diag}}$, any relabelling of the vector indices $\{i\}$ of a solution L_{ij} is also a solution, and it is easily checked that the relabellings are inner automorphic in $SO(n)$. A solution L is said to have a symmetry when one or more inner automorphisms act trivially on L. It follows that

$$\text{auto } L = \{\text{non-trivial relabellings of vector indices in } \{L_{ij}\}\} \tag{2.29}$$

and $\dim(\text{auto } L) \leqq n!$, the equality being attained when the solution has no symmetry. A representative of each automorphism cycle is obtained by choosing a particular labelling in each auto L.

8. Conformal weights. The L^{ab}-broken conformal weights of the integrable representation T_a are the eigenvalues of $\Delta = L^{ab}T_aT_b$ [12, 18]. The result

$$\Delta_i = \frac{\tau}{2} \sum_{k \neq i}^{n} L_{ki}, \qquad 1 \leqq i \leqq n \tag{2.30}$$

is obtained for the n conformal weights Δ_i of the vector representation $(T_{ij})_{IJ} = i(\delta_{iI}\delta_{jJ} - \delta_{jI}\delta_{iJ})\sqrt{\tau\psi^2/2}$ in $SO(n)_{\text{diag}}$.

2.3. High-Level Expansion and Unitarity. We discuss the high-level expansion [22]

$$L_{ij} = \frac{1}{x} \sum_{p=0}^{\infty} L_{ij}^{(p)} x^{-p}, \qquad c = \sum_{p=0}^{\infty} c_p x^{-p} \tag{2.31}$$

of the master equation (2.21) in the diagonal ansatz. The zeroth order solution is

$$L_{ij}^{(0)}=\theta_{ij}, \quad \theta_{ij}=0 \text{ or } 1, \quad 1 \leqq i \neq j \leqq n \tag{2.32}$$

and the moments of order $p \geqq 1$ are unambiguously computed from the recursion relation

$$L_{ij}^{(p)}=(1-2\theta_{ij})\left\{\sum_{q=1}^{p-1} L_{ij}^{(q)} L_{ij}^{(p-q)} + \tau \sum_{l \neq i,j}^{n}\left[\sum_{q=0}^{p-1}\left(L_{ij}^{(q)}\left(L_{il}^{(p-q-1)}+L_{jl}^{(p-q-1)}\right)-L_{il}^{(q)} L_{lj}^{(p-q-1)}\right)\right]\right\} \tag{2.33a}$$

$$c_p=\sum_{i<j} L_{ij}^{(p)}. \tag{2.33b}$$

The results

$$L_{ij}=\frac{\theta_{ij}}{x}+\frac{L_{ij}^{(1)}}{x^2}+\mathcal{O}(x^{-3}), \quad c=\sum_{i<j}\theta_{ij}+\frac{1}{x}\sum_{i<j} L_{ij}^{(1)}+\mathcal{O}(x^{-2}),$$
$$L_{ij}^{(1)}=-\tau \sum_{l \neq i,j}^{n}\left[\theta_{ij}(\theta_{il}+\theta_{jl})+(1-2\theta_{ij})\theta_{il}\theta_{lj}\right] \tag{2.34}$$

are obtained through order $p=1$.

Important features of the high-level expansion in this case are:

1. Each high-k smooth solution in $SO(n)_{\text{diag}}$ may be unambiguously labelled by the values $\{\theta_{ij}\}$ of its zero[th] order radial variables,

$$L_{ij}(\{\theta_{ij}\}) \leftrightarrow \{\theta_{ij}\}. \tag{2.35}$$

This distinguishes $2^{\binom{n}{2}}$ high-k smooth constructions in $SO(n)_{\text{diag}}$, in agreement with the generic counting in (2.22). $SO(n)_{\text{diag}}$ may also contain sporadic solutions at particular levels, which are inaccessible to high-level analysis (see Appendix B).

2. The moments $L_{ij}^{(p)}$ are real to all orders, so that, according to Eq. (2.23) each high-k smooth construction in $SO(n)_{\text{diag}}$ is "unitary to all orders." More precisely, the reality of $L_{ij}^{(p)}$ guarantees unitarity within the radius of convergence of the high-level expansion. Since there is no reason to suspect a zero radius of convergence [18, 20–22], we conjecture that all the high-k smooth solutions in $SO(n)_{\text{diag}}$ are unitary down to some finite critical level. The conjecture is true for the exact new constructions in Sect. 7, whose critical levels, in accord with [18, 21, 22], are quite low.

3. Graph Theory and $SO(n)_{\text{diag}}$

3.1. Graph Rules. According to Eq. (2.35), it is natural to represent each high-k smooth construction $L(\{\theta_{ij}\})$ in $SO(n)_{\text{diag}}$ by a *labelled graph*[4] G,

each high-k smooth solution in $SO(n)_{\text{diag}} \leftrightarrow$ each labelled graph G_n of order n

$$L(G_n) \leftrightarrow G_n \tag{3.1}$$

[4] A labelled graph of order n is a collection of n labelled points (vertices) and a set of undirected lines (edges) which connect distinct points such that no more than one line connects any two points. The number $2^{\binom{n}{2}}$ of (high-k smooth) solutions in $SO(n)_{\text{diag}}$ is equal to the number of labelled graphs of order n [25]

whose set of points $V(G) \equiv \{i\}$ and (undirected) lines $E(G) \equiv \{(ij)\}$ is obtained by the *graph rules*:

$$SO(n) \text{ vector indices } i \leftrightarrow \text{points } i \text{ in graph } G$$
$$\theta_{ij} = 1 \leftrightarrow \text{line between points } i \text{ and } j \text{ in } G\,. \tag{3.2}$$

An immediate consequence is the high-level form

$$T(L(G)) \sim \frac{1}{x\psi^2} \sum_{(ij) \in E(G)} {}^*_*(J_{ij})^2{}^*_* \tag{3.3}$$

of the Virasoro operator of each high-k smooth construction $L(G)$ in $SO(n)_{\text{diag}}$.

In our discussion of graph theory below, the qualifier "high-k smooth" is implicitly assumed when we refer to constructions in $SO(n)_{\text{diag}}$.

3.2. Affine-Virasoro Constructions as Graph Functions. Each affine-Virasoro construction L^{ab} in $SO(n)_{\text{diag}}$ is computable in principle, through the master equation, as a graph function $L^{ab}(G)$ on its graph G. As an example, we have computed the first two moments of the central charge $c(G)$,

$$c_0(G) = \dim E(G) = \frac{1}{2} \sum_i d_i(G)\,, \tag{3.4a}$$

$$c_1(G) = \tau\left(-\frac{3}{2}\sum_i d_i(G)(d_i(G)-1) + 6t_3\right) \leqq 0 \tag{3.4b}$$

for any graph G, using Eqs. (2.31) and (2.34). Here $d_i(G)$ is the *degree* [5] of point i in G, and t_3 is the number of triangles in G. The inequality in (3.4b) follows from the general result that the asymptotic value c_0 of the central charge is approached from below [22]. Similarly, the high-level $L^{ab}(G)$-broken conformal weights of the vector representation

$$\Delta_i(G) = \frac{\tau \Delta_i^{(0)}(G)}{x} + \mathcal{O}(x^{-2}), \qquad \Delta_i^{(0)}(G) = \frac{d_i(G)}{2}, \qquad i = 1, \ldots, n \tag{3.5}$$

are identified with (2.30) as proportional to the degrees of G.

The leading terms of the inverse inertia tensor are

$$L_{ij}(G) = \begin{cases} x^{-1} + x^{-2}\tau(-(d_i(G) + d_j(G) - 2) + l(i,j)) + \mathcal{O}(x^{-3}), & G \text{ has a line } (ij) \\ 0 - x^{-2}\tau l(i,j) + \mathcal{O}(x^{-3}), & G \text{ has no line } (ij) \end{cases}, \tag{3.6}$$

where $l(i,j)$ is the number of points $l \neq i,j$ in G which are connected to both of the points i and j. More generally, the exact result

$$L_{ij}(G) = 0 \text{ when } G \text{ has no path of any length from } i \text{ to } j \tag{3.7}$$

is obtained to all orders from the recursion relation (2.33a).

The result (3.7) implies a physical characterization of the disconnected graphs: A graph is *connected* if each distinct pair of points is connected by some path of lines, and disconnected otherwise. Examples are given in Fig. 1. Each disconnected graph is the *union* $G_1 \cup G_2 \cup \ldots \cup G_N$ (see Fig. 1) of some set of connected graphs $\{G_i\}$. It follows from the result (3.7) that the disconnected graphs are reducible constructions (see Sect. 2.2) with commuting Virasoro operators $T(L(G_i))$.

[5] The degree $d_i(G) = \sum_{k \neq i} \theta_{ik}$ of point i is the number of lines attached to the point [25]

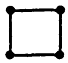

a

b

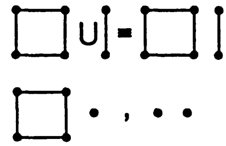

Fig. 1. a Connected graphs; **b** Disconnected graphs

3.3. Automorphisms and Isomorphisms. The automorphism cycles of $SO(n)_{\text{diag}}$ are easily understood in graph theory. Two graphs are isomorphic when they differ by a relabelling of their points. The particular relabellings of a graph G which preserve the same set of lines $\{\theta_{ij}=1\}$ form a group auto G of (graph) automorphisms (or trivial isomorphisms) of the graph. Physically, auto G is the symmetry group of the graph G. It follows from our discussion in Sect. 2.2 that

$$SO(n) \text{ automorphisms} = \text{graph isomorphisms}, \tag{3.8a}$$

$$\text{auto } L(G) = \{\text{non-trivial isomorphisms of } G\}, \tag{3.8b}$$

$$1 \text{ representative of auto } L(G) \leftrightarrow 1 \text{ unlabelled graph } G, \tag{3.8c}$$

and, more physically, that

$$\begin{aligned}&\text{each physically distinct affine-Virasoro construction in } SO(n)_{\text{diag}}\\ &\qquad \leftrightarrow \text{each unlabelled graph of order } n.\end{aligned} \tag{3.9}$$

This one-to-one correspondence describes an immense structure in $SO(n)_{\text{diag}}$, which is itself much smaller than the space of all solutions on $SO(n)$.

It also follows from (3.8b) that the dimension of the $SO(n)$ automorphism cycle of a construction $L(G_n)$ in $SO(n)_{\text{diag}}$ is equal to the number of non-trivial isomorphisms of G_n, so that

$$\dim(\text{auto}\, L(G_n)) = \frac{n!}{S(G_n)}, \tag{3.10}$$

where $S(G) \equiv \dim(\text{auto}\, G)$ is the *symmetry factor*[6] of the graph. The related, but somewhat more technical conclusion

$$\text{symmetry group of } L(G) = \text{auto}\, G \tag{3.11}$$

will be established in Sect. 6.

We employ only *unlabelled graphs* below, unless stated otherwise, as representatives of the physically distinct conformal field theories.

3.4. Affine-Sugawara Nested Graphs. In this section, we identify the graphs of the affine-Sugawara nests in $SO(n)_{\text{diag}}$.

1. Affine-Sugawara graphs. These are the graphs of order $n \geqq 1$ with all possible lines

$$\begin{aligned}K_n &= \text{complete graph on } n \text{ points}\\ &= \text{affine-Sugawara construction on } SO(n)\end{aligned} \tag{3.12}$$

---

[6] The basic composition law for symmetry factors is $S(G_1 \cup G_2) = \zeta S(G_1) S(G_2)$, where $\zeta = 2$ when $G_1 = G_2$ and $\zeta = 1$ otherwise

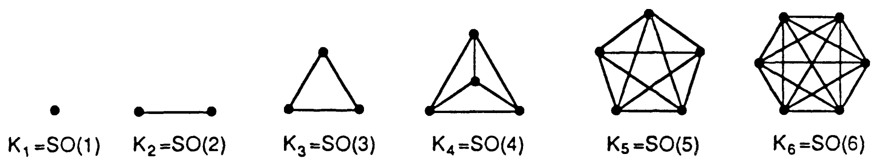

Fig. 2. Complete graphs = affine-Sugawara constructions = fundamental affine-Sugawara nests of depth 1

shown for $1 \leqq n \leqq 6$ in Fig. 2. The affine-Sugawara graphs are the most symmetric connected graphs, with $\operatorname{auto} K_n = S_n$, $\dim(\operatorname{auto} K_n) = n!$ and $\dim(\operatorname{auto} L(K_n)) = 1$. The composition law for affine-Sugawara graphs

$$G(SO(n)) = K_n, \qquad G(SO(m) \times SO(n)) = K_m \cup K_n \tag{3.13}$$

will be useful below.

2. K-conjugate graphs. The high-level form of K-conjugation in $SO(n)_{\text{diag}}$

$$\theta_{ij} \to \tilde{\theta}_{ij} = 1 - \theta_{ij}, \qquad c_0 \to \tilde{c}_0 = \binom{n}{2} - c_0 \tag{3.14}$$

is obtained from (2.24). For each graph G_n of order n, the map (3.14) defines a K-conjugate graph [7] $\tilde{G}_n$ on $SO(n)$,

$$\tilde{G}_n : V(\tilde{G}_n) = V(G_n), \qquad E(\tilde{G}_n) = E(K_n) - E(G_n), \tag{3.15}$$

which represents the K-conjugate theory

$$L(\tilde{G}_n) \equiv \tilde{L}(G_n) = L(K_n) - L(G_n) \tag{3.16}$$

of the theory $L(G_n)$. The degrees of $\tilde{G}_n$ satisfy $d_i(\tilde{G}_n) = n - 1 - d_i(G_n)$.

As illustrated in Fig. 3, the K-conjugate graph $\tilde{G}_n$ is obtained on the points of G_n by removing the lines of G_n from the affine-Sugawara graph K_n. It follows that $\tilde{K}_n$ is the totally disconnected graph of order n, such that $L(\tilde{K}_n) = \tilde{L}(K_n) = 0$ is the trivial construction on $SO(n)$, and $\tilde{K}_1 = K_1$ is the trivial graph. It is also clear that

$$\begin{gathered} \operatorname{auto} G = \operatorname{auto} \tilde{G}, \\ \dim(\operatorname{auto} L(G)) = \dim(\operatorname{auto} L(\tilde{G})) \end{gathered} \tag{3.17}$$

since K-conjugation is a 1-1 map.

[7] The K-conjugate graph $\tilde{G}$ of a graph G is called $\tilde{G} = \bar{G}$, the *complement* of G, in the literature of graph theory

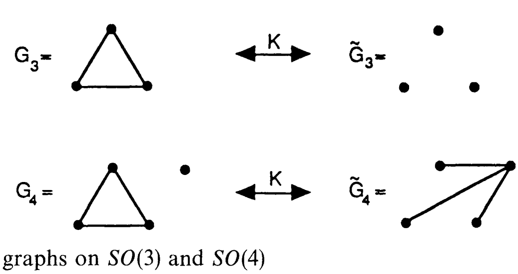

Fig. 3. K-conjugate graphs on $SO(3)$ and $SO(4)$

3. Subgroup and fundamental coset graphs. The subgroup graphs in $SO(n)_{\text{diag}}$

$$G(h(SO(n)_{\text{diag}})) = K_{m_1} \cup K_{m_2} \cup \ldots \cup K_{m_N}$$
$$\sum_{i=1}^{N} m_i = n, \quad 2 \leqq N \leqq n-1, \quad m_i \geqq 1 \tag{3.18}$$

are obtained from $h(SO(n)_{\text{diag}})$ in (2.25) with the composition law (3.13). The subgroup graphs are disconnected graphs of order n because of the range restrictions on $\{m_i\}$.

The fundamental coset graphs of the fundamental coset constructions $SO(n)/h(SO(n)_{\text{diag}})$ are obtained by K-conjugation of the subgroup graphs in (3.18). A useful identity is

$$\widetilde{G_1 \cup G_2} = \tilde{G}_1 + \tilde{G}_2 \tag{3.19}$$

where the *join* $G_1 + G_2$ of two graphs is defined by connecting every point in G_1 to every point in G_2. It follows that the fundamental coset graphs of $SO(n)_{\text{diag}}$ are the connected graphs

$$G(SO(n)/h(SO(n)_{\text{diag}})) = \tilde{G}(h(SO(n)_{\text{diag}})) = \tilde{K}_{m_1} + \tilde{K}_{m_2} + \ldots + \tilde{K}_{m_N}. \tag{3.20}$$

In graph theory, the *complete N-partite graphs* are obtained in this way as the join of $N \geqq 2$ totally disconnected graphs. It follows that the affine-Sugawara graphs K_n are the complete N-partite graphs of order $n = N$, and that

$$\text{fundamental coset graphs in } SO(n)_{\text{diag}}$$
$$= \text{complete } N\text{-partite graphs of order } n > N. \tag{3.21}$$

Figure 4 contains a representation of general complete bipartite (2-partite) and 3-partite graphs. In these representations, each circle, called a *lacuna* of the graph, contains one of the totally disconnected graphs $\tilde{K}_{m_i}$ in (3.20). The lines of the graphs connect all points in distinct lacunae.

4. Affine-Sugawara nested graphs. The fundamental affine-Sugawara nested graphs $G(\mathcal{N}_n(d))$ of depth d are the graphs of the fundamental affine-Sugawara nests $\mathcal{N}_n(d)$. The affine-Sugawara graphs in Fig. 2 and the fundamental coset graphs in Fig. 4 are the fundamental affine-Sugawara nested graphs of depth 1 and 2 respectively.

Physically, the fundamental coset graphs in Fig. 4 are formed by *removal* ($\ominus$) of subgroup graphs from the complete affine-Sugawara graph. More generally, the fundamental nested graphs at depth d are formed by removal of fundamental

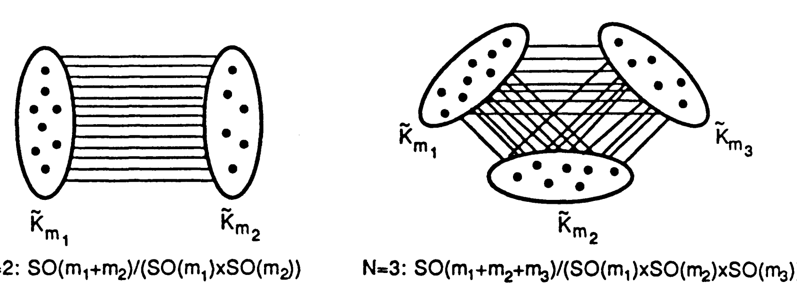

Fig. 4. Complete N-partite graphs = fundamental coset constructions = fundamental affine-Sugawara nests of depth 2

nested graphs of depth $d-1$ on smaller manifolds from the affine-Sugawara graph:

$$G(\text{nest of depth } d) = G\left(\frac{\text{Sugawara}}{\text{nest of depth } d-1}\right)$$
$$= G(\text{Sugawara}) \ominus G(\text{nest of depth } d-1)\,. \tag{3.22}$$

Alternately, we may think of the nested graphs at depth d as formed by *insertion* ($\ominus\ominus$) of fundamental nested graphs of depth $d-2$ into the fundamental coset graphs

$$G(\text{nest of depth } d) = G\left(\frac{\dfrac{\text{Sugawara}}{\text{subgroups}}}{\text{nest of depth } d-2}\right)$$
$$= G(\text{cosets}) \ominus \ominus G(\text{nest of depth } d-2) \tag{3.23}$$

since the nest of depth $d-2$ is itself removed from the subgroups.

A precise definition of this recursive structure is

$$\begin{aligned}
&\text{fundamental affine-Sugawara nested graphs of depth } d \geqq 3\\
&\quad = \text{fundamental coset graphs with insertion of depth } d-2\\
&\quad \equiv \begin{cases} \text{graphs built by insertion of at least one fundamental affine-}\\ \text{Sugawara nested graph of depth } d-2\text{, and any number}\\ \text{of affine-Sugawara nested graphs of depth } \leqq d-2\text{,}\\ \text{in the lacunae of complete } N\text{-partite graphs.} \end{cases}
\end{aligned} \tag{3.24}$$

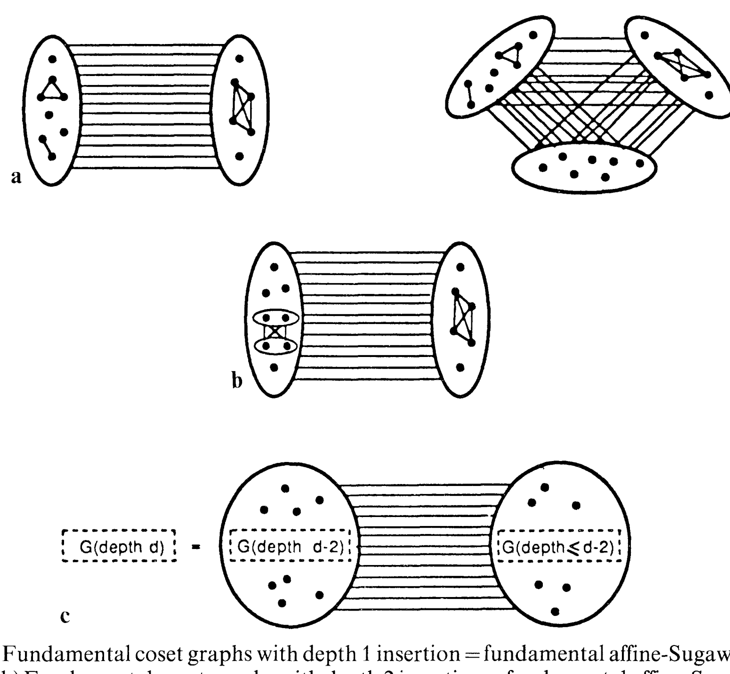

Fig. 5. a) Fundamental coset graphs with depth 1 insertion = fundamental affine-Sugawara nests of depth 3; b) Fundamental coset graphs with depth 2 insertion = fundamental affine-Sugawara nests of depth 4; c) Fundamental coset graphs with depth $d-2$ insertion = fundamental affine-Sugawara nests of depth d

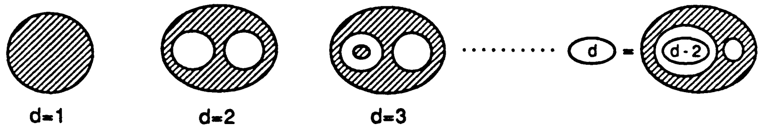

Fig. 6. Complementary representation of fundamental affine-Sugawara nested graphs

Insertion of a nested graph in a lacuna of the same order is not allowed. Figure 5a shows two fundamental affine-Sugawara nested graphs of depth 3, obtained from the coset graphs of Fig. 4 by insertion of depth one affine-Sugawara graphs in their lacunae. Figure 5b is a fundamental nested graph of depth 4, obtained from a coset graph by inserting another depth 2 coset graph in one of its lacunae[8]. The graphical form of the recursive definition (3.24) is given in Fig. 5c.

The last form of the definition (3.24) and the schematic representation of the fundamental affine-Sugawara nested graphs in Figs. 4 and 5 are designed to exhibit the N-partite structure of the nests, since we will see below that the $N=2$ nests play a special role. The complementary representation in Fig. 6 shows the nested graphs as an alternating subtraction (open areas) or addition (shaded areas) of the lines of affine-Sugawara graphs. The bottom of each nest is the set of innermost open and shaded areas. For example, the bottom of the depth-two nest consists of two open areas, which records that two smaller affine-Sugawara graphs have been removed. The open spaces of this representation are not the lacunae of complete N-partite graphs, however, since the spaces do not contain all the points of the graphs.

The fundamental affine-Sugawara nested graphs $G(\mathcal{N}_n(d))$ are always connected graphs of order n, while the K-conjugate nested graphs $\tilde{G}(\mathcal{N}_n(d))$ are always disconnected[9] graphs of order n. Together, they form the set of *affine-Sugawara nested graphs*, which contains all known rational constructions in $SO(n)_{\mathrm{diag}}$.

3.5. Affine-Virasoro Nested Graphs. The more general fundamental affine-Virasoro nested graphs are the graphs of the fundamental affine-Virasoro nests, defined in Sect. 2.2. These graphs retain the subgroup nesting structure in Fig. 6 of the fundamental affine-Sugawara nested graphs, now allowing general graphs at the bottom of the nest. Together, the fundamental affine-Virasoro nested graphs and their K-conjugate graphs form the set of all *affine-Virasoro nested graphs*, which includes all graphs.

3.6. Irreducible Graphs. A graph G is called *(ir)reducible* if $L(G)$ is an (ir)reducible construction in $SO(n)_{\mathrm{diag}}$ (see Sect. 2.2). (Ir)reducible graphs are characterized as follows.

Disconnected graphs are always the unions of graphs on smaller manifolds, so it follows from our discussion in Sect. 2.2 that disconnected graphs are always reducible graphs, and hence that irreducible graphs are always connected. We also know from Sect. 2.2 that a) the affine-Sugawara graph is the only irreducible affine-

[8] Algebraically, the first four nest depths show the alternating pattern: $G(\mathcal{N}_n(1))=K_n$, $G(\mathcal{N}_n(2)) =\{+\tilde{K}\}$, $G(\mathcal{N}_n(3))=\{+\cup K\}$ and $G(\mathcal{N}_n(4))=\{+\cup+\tilde{K}\}$, where the order of the K's and $\tilde{K}$'s may vary from 1 to $n-1$. More generally, the $d\to d+1$ operations $K\to+\tilde{K}$ (d odd) and $\tilde{K}\to\cup K$ (d even) generate the algebraic form of the fundamental nests at arbitrary depth

[9] The K-conjugate graphs $\tilde{G}(\mathcal{N}_n(d))=G(\tilde{\mathcal{N}}_n(d))$ of the fundamental affine-Sugawara nested graphs $G(\mathcal{N}_n(d))$ are unions of fundamental affine-Sugawara nested graphs of lower order

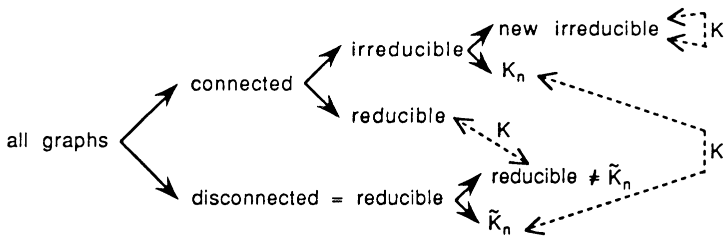

Fig. 7. Irreducible and reducible graphs in graph space. The dashed lines indicate the action of K-conjugation on the graphs of each category

Sugawara nested graph on each manifold and b) the *new irreducible graphs* G are those for which both G and $\tilde{G}$ are irreducible, and hence connected.

This establishes the characterization

$$G \text{ is a new irreducible graph iff } G \text{ and } \tilde{G} \text{ are both non-trivial connected graphs} \tag{3.25}$$

since K_1 is the only irreducible graph on $SO(1)$. The characterization (3.25) is a useful tool in the identification of new constructions below. Figure 7 displays a more complete map of irreducible and reducible graphs in graph space.

Irreducible graphs are important because graph space may be organized as the set of fundamental affine-Virasoro nested graphs with irreducible graphs at the bottom of each nest, plus the K-conjugates of these graphs (see Sect. 2.2).

3.7. Counting Old and New Constructions. We consider the following basic numbers

$$\begin{aligned} g_n &\equiv \text{number of all graphs of order } n \\ C_n &\equiv \text{number of connected graphs of order } n \\ C(AS)_n &\equiv \begin{cases} \text{number of connected (fundamental)} \\ \text{affine-Sugawara nested graphs of order } n\,. \end{cases} \end{aligned} \tag{3.26}$$

The first two numbers are known in graph theory [24], and the recursion relation

$$C(AS)_n = 2C(AS)_{n-1} + \sum_{\{p(i)\}} \prod_{\substack{i=2 \\ p(i)\neq 0}}^{n-2} \binom{p(i)+C(AS)_i - 1}{p(i)}, \qquad c(AS)_2 = 1\,,$$

$$\{p(i) \geqq 0\} \text{ are the partitions of } n = \sum_{i=2}^{n-2} ip(i) \tag{3.27}$$

is derived in Appendix A. Other numbers of interest [10]

$$\begin{aligned} D_n &\equiv \text{number of disconnected graphs of order } n \\ &= g_n - C_n\,, \\ g(AS)_n &\equiv \text{number of affine-Sugawara nested graphs of order } n \\ &= 2C(AS)_n\,, \end{aligned}$$

[10] The connected (fundamental) affine-Sugawara nested graphs $G(\mathcal{N}_n(d))$ are in 1-1 correspondence with the disconnected affine-Sugawara nested graphs $\tilde{G}(\mathcal{N}_n(d))$ by K-conjugation (see Sect. 3.4)

Table 1. Connected constructions in $SO(n)_{\mathrm{diag}}$

Manifold $SO(n)_{\mathrm{diag}}$	All constructions g_n	Connected constructions C_n	Fundamental affine-Sugawara nests $C(AS)_n$	New connected constructions $C_n^{\#}$
$SO(1)$	1	1	1	0
$SO(2)$	2	1	1	0
$SO(3)$	4	2	2	0
$SO(4)$	11	6	5	1
$SO(5)$	34	21	12	9
$SO(6)$	156	112	33	79
$SO(7)$	1,044	853	90	763
$SO(8)$	12,346	11,117	261	10,856
$SO(9)$	274,668	261,080	766	260,314
$SO(10)$	12,005,168	11,716,571	2,312	11,714,259

$$\begin{aligned} D(AS)_n &\equiv \text{number of disconnected affine-Sugawara nested graphs of order } n \\ &= C(AS)_n\,, \\ C_n^{\#} &\equiv \text{number of new connected constructions of order } n \\ &= C_n - C(AS)_n \end{aligned} \tag{3.28}$$

are expressed in terms of the basic numbers (3.26). The values of g_n, C_n, $C(AS)_n$, and $C_n^{\#}$ are given for $1 \leqq n \leqq 10$ in Table 1.

The results of Table 1 show a dramatic dominance of connected new constructions over connected known constructions as n increases. Similar behavior is observed for $g_n^{\#} \equiv g_n - g(AS)_n$ and $g(AS)_n$ when disconnected graphs are included. The asymptotic results [11]

$$C_n \sim g_n = \mathcal{O}(e^{n^2(\ln 2)/2})\,, \qquad SO(n \gg 1) \tag{3.29a}$$

$$C(AS)_n = g(AS)_n/2 \leqq \mathcal{O}(e^{2n \ln 2})\,, \qquad SO(n \gg 1) \tag{3.29b}$$

are a quantitative statement of the dominance of new over old constructions in $SO(n)_{\mathrm{diag}}$. The asymptotic bound (3.29b) on the number of fundamental affine-Sugawara nests in $SO(n)_{\mathrm{diag}}$ is obtained in Appendix A. The corresponding characterization

$$\text{the generic graph in } SO(n \gg 1)_{\mathrm{diag}} \text{ is a new connected construction} \tag{3.30}$$

follows immediately from (3.29).

A fundamental measure of new and old constructions is provided by the irreducible graphs, whose definition, loosely speaking, mods out by the affine-Virasoro nesting (see Sects. 2.2 and 3.6). These graphs are counted as follows. At order n, define ir_n, $\mathrm{ir}(AS)_n$, and $\mathrm{ir}_n^{\#}$ as the total number of irreducible graphs and the number of old and new irreducible graphs respectively. Then we know that

$$\mathrm{ir}(AS)_n = 1\,, \qquad \mathrm{ir}_n = \mathrm{ir}_n^{\#} + 1\,, \tag{3.31}$$

[11] It is known in graph theory that the generic large-order graph is connected, and the asymptotic estimate $C_n \sim g_n$ in (3.29a) is given in [24]; The exponential order of g_n is the exponential order of the number $2^{\binom{n}{2}}$ of solutions in $SO(n)_{\mathrm{diag}}$, since auto $L(G)$ is combinatoric and hence factorial

Table 2. Irreducible constructions in $SO(n)_{\text{diag}}$

Manifold $SO(n)_{\text{diag}}$	Total irreducible constructions ir_n	Irreducible affine-Sugawara nests $ir(AS)_n$	New irreducible constructions $ir_n^{\#}$
$SO(1)$	1	1	0
$SO(2)$	1	1	0
$SO(3)$	1	1	0
$SO(4)$	2	1	1
$SO(5)$	9	1	8
$SO(6)$	69	1	68
$SO(7)$	663	1	662
$SO(8)$	9,889	1	9,888
$SO(9)$	247,493	1	247,492
$SO(10)$	11,427,975	1	11,427,974

since the affine-Sugawara graph K_n is the only irreducible affine-Sugawara nested graph on $SO(n)$. It follows from Fig. 7 that

$$\mathrm{ir}_n = C_n - C(\mathrm{red})_n\,, \tag{3.32a}$$

$$C(\mathrm{red})_n = D_n - 1 = g_n - C_n - 1\,, \tag{3.32b}$$

where $C(\mathrm{red})_n$ is the number of connected reducible graphs in $SO(n)_{\text{diag}}$. The last form in (3.32b) follows with $D_n = g_n - C_n$. The result for new irreducible graphs[12]

$$\mathrm{ir}_n^{\#} = 2C_n - g_n \tag{3.33}$$

is then obtained from Eqs. (3.31) and (3.32).

Numerical values of ir_n, $\mathrm{ir}(AS)_n$, and $\mathrm{ir}_n^{\#}$ are given for $1 \leqq n \leqq 10$ in Table 2, which shows that the dominance of new over old constructions in $SO(n)_{\text{diag}}$ is even more dramatic after moding out the nests. The asymptotic behavior of the irreducible graphs

$$\mathrm{ir}_n^{\#} \sim \mathrm{ir}_n \sim C_n \sim g_n = \mathcal{O}(e^{n^2(\ln 2)/2}) \tag{3.34}$$

is obtained from Eqs. (3.29a) and (3.33), and, finally, the characterization

$$\text{the generic graph in } SO(n \gg 1)_{\text{diag}} \text{ is a new irreducible construction} \tag{3.35}$$

follows from this behavior.

4. Application to $SO(n \leqq 6)_{\text{diag}}$

Table 3 lists the unlabelled graphs of order 6, which are the physically distinct constructions in $SO(6)_{\text{diag}}$. The table can be used for $SO(n<6)$ as well, since the constructions with m trivial subgraphs appear first, without the trivial subgraphs, as constructions in $SO(6-m)_{\text{diag}}$. The following data are given:

1. The graphs G of the high-level sector numbers $0 \leqq c_0 = \dim E(G) \leqq 7$.

[12] $C_n \geqq D_n$ is a consequence of the result (3.33), since the number of new irreducible graphs is non-negative

2. The automorphism group auto$G$ of each graph, e.g. $Z_2 \times S_3$ for $SO(6)/SO(5)/SO(2)$ in sector 6.

3. The dimension of the $SO(6)$ automorphism cycle dim(auto$L(G)$), computed from Eq. (3.10).

4. The conformal field-theoretic name of each construction. The affine-Sugawara nested graphs are identified from their N-partite characterization in Sect. 3.4. Figures 8a and 8b show examples of the translation from the symmetrically-drawn graphs of the table to the N-partite forms. The remaining new construc-

Table 3. The graphs of $SO(6)_{\text{diag}}$

c_0	G	auto G	dim auto L(G)	conformal construction L(G)	$\{2\Delta_i^{(0)}\}$	$\tilde{G}$
0	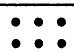	S_6	1	L=0	(0,0,0,0,0,0)	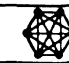
1	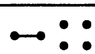	$Z_2 x S_4$	15	SO(2)	(0,0,0,0,1,1)	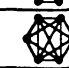
2	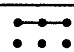	$Z_2 x S_3$	60	SO(3)/SO(2)	(0,0,0,1,1,2)	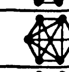
	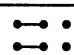	$(Z_2)^4$	45	$(SO(2))^2$	(0,0,1,1,1,1)	
3	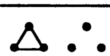	$S_3 x S_3$	20	SO(3)	(0,0,0,2,2,2)	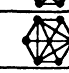
	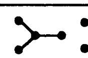	$S_3 x Z_2$	60	SO(4)/SO(3)	(0,0,1,1,1,3)	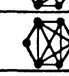
	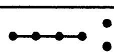	$Z_2 x Z_2$	180	$SO(4)^{\#}[d,4]$	(0,0,1,1,2,2)	
	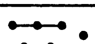	$Z_2 x Z_2$	180	(SO(3)/SO(2))xSO(2)	(0,1,1,1,1,2)	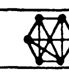
		$(Z_2)^3 x S_3$	15	$(SO(2))^3$	(1,1,1,1,1,1)	
4	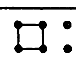	$D_4 x Z_2$	45	$SO(4)/(SO(2))^2$	(0,0,2,2,2,2)	
	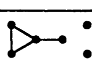	$Z_2 x Z_2$	180	SO(4)/SO(3)/SO(2)	(0,0,1,2,2,3)	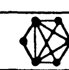
	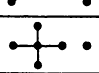	S_4	30	SO(5)/SO(4)	(0,1,1,1,1,4)	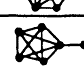
	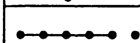	Z_2	360	$SO(5)^{\#}[d,6]_2$	(0,1,1,2,2,2)	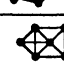
	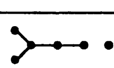	Z_2	360	$SO(5)^{\#}[d,7]_1$	(0,1,1,1,2,3)	
	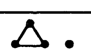	$S_3 x Z_2$	60	SO(3)xSO(2)	(0,1,1,2,2,2)	
	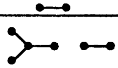	$S_3 x Z_2$	60	(SO(4)/SO(3))xSO(2)	(1,1,1,1,1,3)	
	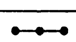	$(Z_2)^3$	90	$(SO(3)/SO(2))^2$	(1,1,1,1,2,2)	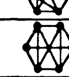
	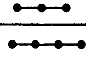	$Z_2 x Z_2$	180	$SO(4)^{\#}[d,4]xSO(2)$	(1,1,1,1,2,2)	

Table 3 (continued)

c_0	G	auto G	dim auto L(G)	conformal construction L(G)	$\{2\Delta_i^{(0)}\}$	$\tilde{G}$
5	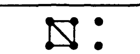	$(Z_2)^3$	90	SO(4)/SO(2)	(0,0,2,2,3,3)	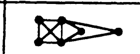
	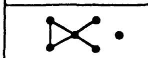	$Z_2 x Z_2$	180	SO(5)/SO(4)/SO(2)	(0,1,1,2,2,4)	
	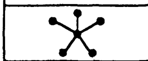	S_5	6	SO(6)/SO(5)	(1,1,1,1,1,5)	
	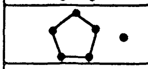	D_5	72	$SO(5)^{\#}[d,2]$	(0,2,2,2,2,2)	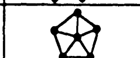
	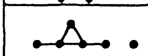	Z_2	360	$SO(5)^{\#}[d,6]_1$	(0,1,1,2,3,3)	
	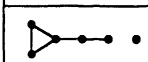	Z_2	360	$SO(5)^{\#}[d,7]_2$	(0,1,2,2,2,3)	
	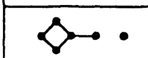	Z_2	360	$SO(5)/SO(5)^{\#}[d,7]_2$	(0,1,2,2,2,3)	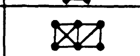
	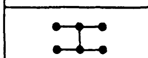	$(Z_2)^3$	90	$SO(6)^{\#}[d,5]_1$	(1,1,1,1,3,3)	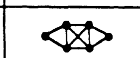
	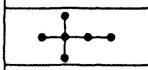	S_3	120	$SO(6)^{\#}[d,7]_1$	(1,1,1,1,2,4)	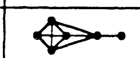
	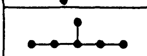	Z_2	360	$SO(6)^{\#}[d,9]_1$	(1,1,1,2,2,3)	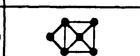
	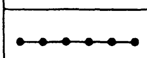	Z_2	360	$SO(6)^{\#}[d,9']_1$	(1,1,2,2,2,2)	
	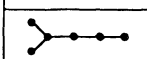	Z_2	360	$SO(6)^{\#}[d,11]_1$	(1,1,1,2,2,3)	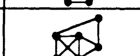
	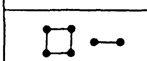	$D_4 x Z_2$	45	$(SO(4)/(SO(2))^2)xSO(2)$	(1,1,2,2,2,2)	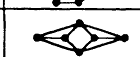
	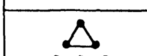	$S_3 x Z_2$	60	(SO(3)/SO(2))xSO(3)	(1,1,2,2,2,2)	
	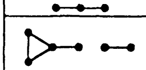	$Z_2 x Z_2$	180	(SO(4)/SO(3)/SO(2))xSO(2)	(1,1,1,2,2,3)	
6	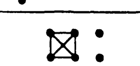	$S_4 x Z_2$	15	SO(4)	(0,0,3,3,3,3)	
	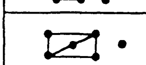	$Z_2 x S_3$	60	SO(5)/(SO(3)xSO(2))	(0,2,2,2,3,3)	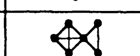
	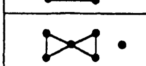	$(Z_2)^3$	90	$SO(5)/SO(4)/(SO(2))^2$	(0,2,2,2,2,4)	
	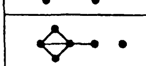	Z_2	360	SO(5)/SO(4)/SO(3)/(SO(2))	(0,1,2,2,3,4)	
	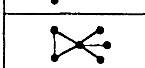	$Z_2 x S_3$	60	SO(6)/SO(5)/SO(2)	(1,1,1,2,2,5)	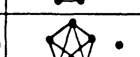

Table 3 (continued)

c_0	G	auto G	dim auto L(G)	conformal construction L(G)	$\{2\Delta_i^{(0)}\}$	$\tilde{G}$
6		Z_2	360	$SO(5)/SO(5)^{\#}[d,6]_2$	(0,2,2,2,3,3)	
		Z_2	360	$SO(5)/SO(5)^{\#}[d,7]_1$	(0,1,2,3,3,3)	
		D_6	60	$SO(6)^{\#}_M \equiv SO(6)^{\#}[d,3]$	(2,2,2,2,2,2)	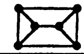
	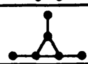	S_3	120	$SO(6)^{\#}[d,4]$	(1,1,1,3,3,3)	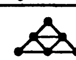
		$Z_2 x Z_2$	180	$SO(6)^{\#}[d,7']_1$	(1,1,2,2,3,3)	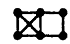
	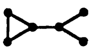	$Z_2 x Z_2$	180	$SO(6)^{\#}[d,8]_1$	(1,1,2,2,3,3)	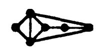
	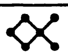	$Z_2 x Z_2$	180	$SO(6)^{\#}[d,8]_2$	(1,1,2,2,2,4)	
	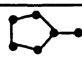	Z_2	360	$SO(6)^{\#}[d,9]_2$	(1,2,2,2,2,3)	
		Z_2	360	$SO(6)^{\#}[d,9']_2$	(1,1,2,2,3,3)	
		Z_2	360	$SO(6)^{\#}[d,11]_2$	(1,2,2,2,2,3)	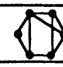
	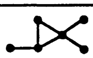	Z_2	360	$SO(6)^{\#}[d,11]_3$	(1,1,1,2,3,4)	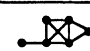
	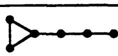	Z_2	360	$SO(6)^{\#}[d,11]_4$	(1,2,2,2,2,3)	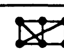
	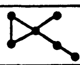	Z_2	360	$SO(6)^{\#}[d,11]_5$	(1,1,2,2,2,4)	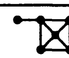
		I	720	$SO(6)^{\#}[d,15]_1$	(1,1,2,2,3,3)	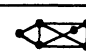
		$(S_3)^2 x Z_2$	10	$(SO(3))^2$	(2,2,2,2,2,2)	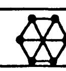
	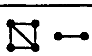	$(Z_2)^3$	90	$(SO(4)/SO(2))xSO(2)$	(1,1,2,2,3,3)	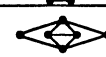
7	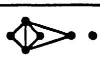	$Z_2 x S_3$	60	$SO(5)/SO(3)$	(0,2,2,2,4,4)	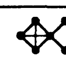
	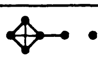	S_3	120	$SO(5)/SO(4)/SO(3)$	(0,1,3,3,3,4)	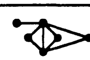
	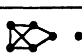	$Z_2 x Z_2$	180	$SO(5)/((SO(3)/SO(2))x(SO(2))$	(0,2,3,3,3,3)	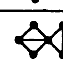
	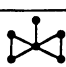	$(Z_2)^3$	90	$SO(6)/SO(5)/(SO(2))^2$	(1,2,2,2,2,5)	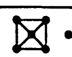

Table 3 (continued)

c_0	G	auto G	dim auto L(G)	conformal construction L(G)	$\{2\Delta_i^{(0)}\}$	$\tilde{G}$
7	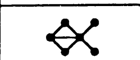	$Z_2 x Z_2$	180	SO(6)/SO(5)/SO(3)/SO(2)	(1,1,2,2,3,5)	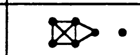
	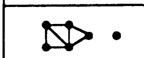	Z_2	360	SO(5)/SO(4)$^{\#}$[d,4]	(0,2,2,3,3,4)	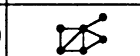
	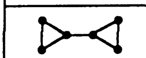	$(Z_2)^3$	90	SO(6)$^{\#}$[d,5]$_2$	(2,2,2,2,3,3)	
	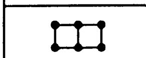	$Z_2 x Z_2$	180	SO(6)$^{\#}$[d,6]	(2,2,2,2,3,3)	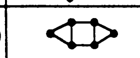
	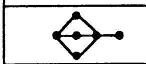	S_3	120	SO(6)$^{\#}$[d,7]$_2$	(1,2,2,2,3,4)	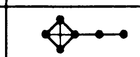
	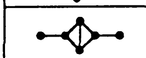	$Z_2 x Z_2$	180	SO(6)$^{\#}$[d,7']$_2$	(1,1,3,3,3,3)	
	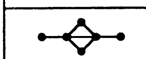	$Z_2 x Z_2$	180	SO(6)$^{\#}$[d,7']$_3$	(1,1,2,2,4,4)	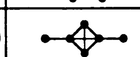
	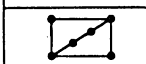	$Z_2 x Z_2$	180	SO(6)$^{\#}$[d,7']$_4$	(2,2,2,2,3,3)	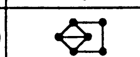
	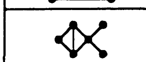	$Z_2 x Z_2$	180	SO(6)$^{\#}$[d,8]$_3$	(1,1,2,3,3,4)	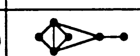
	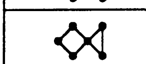	$Z_2 x Z_2$	180	SO(6)$^{\#}$[d,8]$_4$	(2,2,2,2,2,4)	
	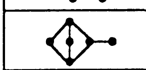	$Z_2 x Z_2$	180	SO(6)$^{\#}$[d,8]$_5$	(1,2,2,3,3,3)	
	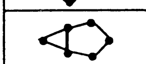	Z_2	360	SO(6)$^{\#}$[d,9]$_3$	(2,2,2,2,3,3)	
	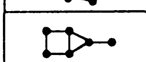	Z_2	360	SO(6)$^{\#}$[d,9]$_4$	(1,2,2,3,3,3)	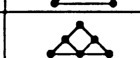
	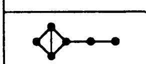	Z_2	360	SO(6)$^{\#}$[d,11]$_6$	(1,2,2,3,3,3)	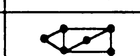
	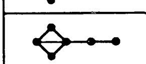	Z_2	360	SO(6)$^{\#}$[d,11]$_7$	(1,2,2,2,3,4)	
	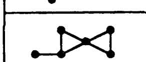	Z_2	360	SO(6)$^{\#}$[d,11]$_8$	(1,2,2,2,3,4)	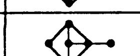
	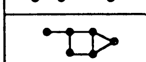	I	720	SO(6)$^{\#}$[d,15]$_2$	(1,2,2,3,3,3)	
	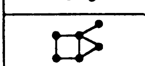	I	720	SO(6)$^{\#}$[d,15]$_3$	(1,2,2,2,3,4)	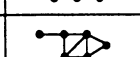
	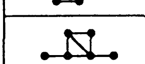	I	720	SO(6)$^{\#}$[d,15]$_4$	(1,1,2,3,3,4)	
	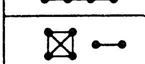	$S_4 x Z_2$	15	SO(4)xSO(2)	(1,1,3,3,3,3)	

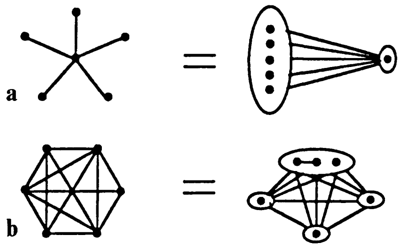

Fig. 8. a) The complete bipartite graph $SO(6)/(SO(5)\times SO(1))=SO(6)/SO(5)$; b) The fundamental affine-Sugawara nested graph $SO(6)/((SO(3)/SO(2))\times(SO(1))^3)=SO(6)/SO(3)/SO(2)$

tions are assigned an $SO(n)^{\#}$ name which also indicates the size of the subansatz in which the construction is found (see Sect. 6).

5. The $L^{ab}(G)$-broken conformal weights $2x\Delta_i(G)\simeq 2\Delta_i^{(0)}=d_i(G)$ of the vector representation at high level.

6. The K-conjugate graph $\tilde{G}$ of each G. These graphs fill the remaining high-level sectors $8\leqq\tilde{c}_0=\dim E(\tilde{G})=15-c_0\leqq 15$, with $\mathrm{auto}\,\tilde{G}=\mathrm{auto}\,G$, $\dim(\mathrm{auto}\,L(\tilde{G}))=\dim(\mathrm{auto}\,L(G))$ and $2\tilde{\Delta}_i^{(0)}=d_i(\tilde{G})=5-d_i(G)$.

In agreement with Table 1, Table 3 shows $g_6=156$ distinct constructions in $SO(6)_{\mathrm{diag}}$, of which $g_n=1$, 2, 4, 11, and 34 constructions appear first in $SO(n)_{\mathrm{diag}}$, $n=1$, 2, 3, 4, and 5. The remaining numbers of Table 1 may also be verified for $n=1,\ldots,6$ from Table 3, and, in particular, there are 90 new constructions in $SO(6)_{\mathrm{diag}}$, of which 79 are connected.

The new irreducible constructions on $SO(n)$ are easily recognized by their name, $SO(n)^{\#}$ or $SO(n)/SO(n)^{\#}$, so that e.g. $SO(4)^{\#}[d,4]\times SO(2)$ in Sect. 4 is reducible on $SO(6)$ while $SO(4)^{\#}[d,4]$ in sector 3 is irreducible on $SO(4)$.

In agreement with Table 2, Table 3 identifies 9 new irreducible constructions in $SO(4)_{\mathrm{diag}}$ and $SO(5)_{\mathrm{diag}}$ [13]

$$\begin{aligned}
&c_0=3:SO(4)^{\#}[d,4]\\
&c_0=5:SO(5)^{\#}[d,2]; \quad c_0=5:SO(5)^{\#}[d,6]_1\\
&c_0=4:SO(5)^{\#}[d,6]_2; \quad c_0=6:SO(5)/SO(5)^{\#}[d,6]_2\\
&c_0=4{,}5:SO(5)^{\#}[d,7]_{1,2}; \quad c_0=6{,}5:SO(5)/SO(5)^{\#}[d,7]_{1,2}\,.
\end{aligned} \tag{4.1}$$

The first five constructions of this list are obtained exactly in Sect. 7. Among the 68 new irreducible constructions in $SO(6)_{\mathrm{diag}}$, the maximal-symmetric constructions [18]

$$\begin{aligned}
c_0=6:SO(6)^{\#}_M&\equiv SO(6)^{\#}[d,3]\\
c_0=9:SO(6)/SO(6)^{\#}_M&\equiv SO(6)/SO(6)^{\#}[d,3]
\end{aligned} \tag{4.2}$$

were identified from the high-level behavior of the known solutions. The exact forms of the next most symmetric constructions

$$c_0=6:SO(6)^{\#}[d,4]; \quad c_0=9:SO(6)/SO(6)^{\#}[d,4] \tag{4.3}$$

are also obtained in Sect. 7.

[13] The first three irreducible constructions in the list (4.1) are examples of self-K-conjugate constructions (see Sect. 5.5)

5. The Graphs $G_n^{\#}$ of $SO(n)_{\text{diag}}^{\#}$

5.1. Identity Graphs. Intuitively, new constructions are less symmetric than old constructions, which are exceptional points with special inertia tensors, commuting currents and so on. Graph theory provides a more quantitative statement of this expectation.

The affine-Sugawara graphs K_n and their K-conjugate graphs $\tilde{K}_n$ are the most symmetric graphs, with symmetry factors $S(K_n)=S(\tilde{K}_n)=n!$. In fact, the affine-Sugawara nested graphs always have at least a Z_2 symmetry, so that their symmetry factors satisfy

$$S(G(\mathcal{N}_n(d)))=S(G(\tilde{\mathcal{N}}_n(d)))\geqq 2\,. \tag{5.1}$$

This argument goes as follows: By repeated application of $\operatorname{auto}G=\operatorname{auto}\tilde{G}$ and $S(G_1\cup G_2\ldots\cup G_N)\geqq\prod_{i=1}^{N}S(G_i)$, the symmetry factor of any affine-Sugawara nest is greater than or equal to the product of symmetry factors of the subgroups at the bottom of the nest, as illustrated in Fig. 10. It follows that, among the affine-Sugawara nests, the chain nest $SO(n)/SO(n-1)/SO(n-2)/\ldots SO(3)/SO(2)$ with $S=S(G(SO(2)))=2$ has the smallest possible symmetry factor.

In contrast, the *identity graphs* I are completely asymmetric with $S(I)=\dim(\operatorname{auto}I)=1$, and they are ubiquitous since the generic large-order graph is an identity graph [24]. It follows that

$$\text{the generic new construction in } SO(n\gg 1)_{\text{diag}}^{\#} \text{ is an identity graph}\,, \tag{5.2a}$$

$$\text{the generic large-order identity graph is a new construction}\,, \tag{5.2b}$$

since the generic large-order graph is also a new construction (see Sect. 3.7). It also follows that constructions with a symmetry are exceptional cases, including those new constructions with $S\geqq 2$.

We have already encountered the first 8 non-trivial identity graphs, collected in Fig. 9, which are identified in Table 3 as new constructions in $SO(6)_{\text{diag}}^{\#}$. Moreover, the characterization

$$\text{all identity graphs are new constructions} \tag{5.3}$$

follows because the affine-Sugawara nested graphs always have a symmetry.

5.2. Connected Incomplete Bipartite Graphs. Connected incomplete bipartite graphs are complete bipartite graphs with one or more lines removed such that the

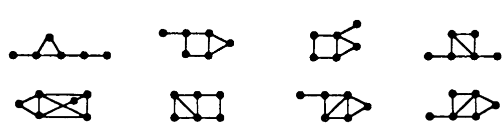

Fig. 9. The first eight identity graphs are new constructions in $SO(6)_{\text{diag}}$

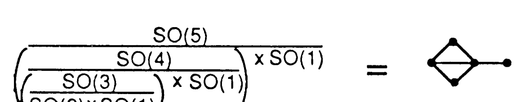

Fig. 10. The symmetry factor of this nests is $S(G(SO(2)\times SO(1)))\cdot S(G(SO(1))\cdot S(G(SO(1))=2$

a
b
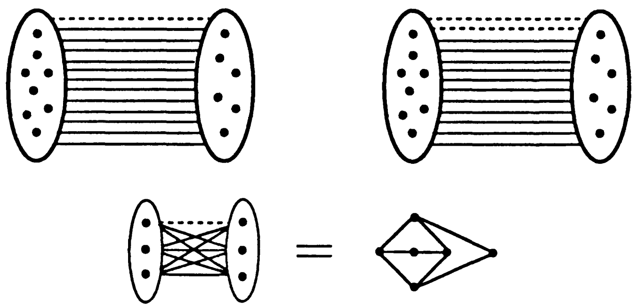

Fig. 11. a Connected incomplete bipartite graphs, or broken $N=2$ coset graphs, are new irreducible constructions. **b** The broken $N=2$ coset graph $SO(6)/SO(6)^{\#}$ $[d, 5]_2$

incomplete graph remains connected. Two examples of these graphs are given in Fig. 11a. The K-conjugate graph $\tilde{G}$ of a connected incomplete bipartite graph G is formed by connecting two affine-Sugawara graphs with one or more lines. It follows from the characterization (3.25) that

$$\text{connected incomplete bipartite graphs are new irreducible constructions,} \tag{5.4}$$

since G and $\tilde{G}$ are both connected in this case.

Physically, the connected incomplete bipartite graphs are the *broken* $N=2$ *coset graphs* obtained by removing lines from the graphs of the fundamental $N=2$ cosets $SO(n)/(SO(p)\times SO(n-p))$. The example in Fig. 11b is identified in Table 3 as a new construction in $SO(6)_{\text{diag}}$.

An equivalent statement of the result (5.4),

$$\text{connected incomplete graphs with } \chi(G)=2 \text{ are new irreducible constructions} \tag{5.5}$$

is obtained in terms of the *chromatic number* [14] $\chi(G)$ of a graph, since a graph is bipartite iff $\chi(G)=2$. As examples, the cycle and path graphs

$$\begin{aligned} C_{2n} &= \text{cycle of length } 2n, \quad n \geqq 3, \\ P_n &= \text{path of length } n-1, \quad n \geqq 4 \end{aligned} \tag{5.6}$$

are new irreducible constructions, as illustrated with the colors r and w in Fig. 12. The cycle C_6 and the paths P_4, P_5, and P_6 are identified as new irreducible constructions in Table 3.

[14] A coloring of a graph G is an assignment of a color to every point in G. The chromatic number $\chi(G)$ is the smallest number of colors such that no two points of the same color are connected by a line [25]

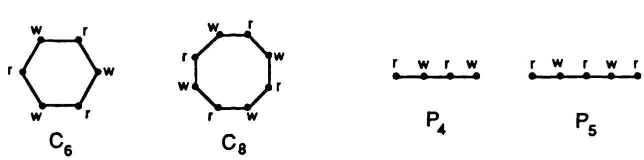

Fig. 12. The cycles C_{2n}, $n\geqq 3$ and paths P_n, $n\geqq 4$ are broken $N=2$ coset graphs and hence new irreducible constructions

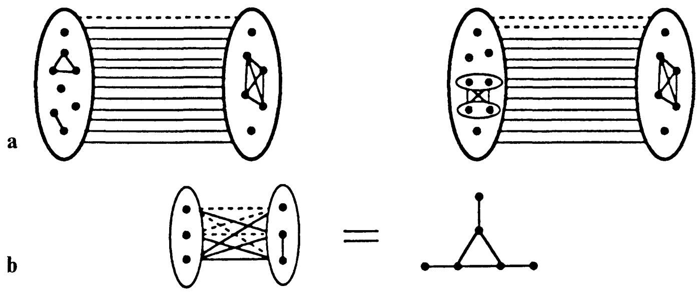

Fig. 13. a Broken $N=2$ affine-Sugawara nested graphs are new irreducible constructions. **b** The broken $N=2$ affine-Sugawara nested graph $SO(6)^{\#}\,[d,4]$

5.3. Broken $N=2$ Affine-Sugawara Nested Graphs. In this section, we introduce the broken $N=2$ affine-Sugawara nested graphs, which generalize the broken $N=2$ coset graphs and which may provide a process which generates all new irreducible graphs from the graphs of the old constructions.

We define the *broken $N=2$ affine-Sugawara nested graphs* as the connected graphs, shown in Figs. 11 and 13, which are obtained by removing lacunae-connecting lines from the fundamental $N=2$ affine-Sugawara nested graphs. The K-conjugate graph $\tilde{G}$ of any broken $N=2$ nest G is also connected since at least one lacunae-connecting line has been removed from G. It follows from the characterization (3.25) that [15]

$$\text{broken } N=2 \text{ affine-Sugawara nested graphs are new irreducible constructions.} \tag{5.7}$$

An example of this result is given in Fig. 13b, which is identified as a new construction in Table 3.

We have also compiled a list of all broken $N=2$ affine-Sugawara nests of order $n \leqq 6$. Comparison of this list with the data of Table 3 supports the complementary conjecture,

$$\begin{aligned}&\text{conjecture 1: At order } n\text{, the set of broken } N=2 \text{ affine-Sugawara nested}\\ &\quad\text{graphs contains } \textit{all} \text{ new irreducible constructions in the lower}\\ &\quad\text{half } 1 \leqq c_0 \leqq \left[\frac{1}{2}\binom{n}{2}\right] \text{ of the high-level sectors of } SO(n)_{\text{diag}}.\end{aligned} \tag{5.8}$$

An implication of this conjecture is that all new irreducible constructions in the upper half of the high-level sectors can be obtained by K-conjugation of the broken nests.

5.4. An Edge Theorem for $SO(n)^{\#}_{\text{diag}}$. It has been observed empirically for the new constructions (1.2) that [22]

$$\begin{gathered}\operatorname{rank} g < c_0 < \dim g - \operatorname{rank} g\\ \text{when } g^{\#} \text{ is a new irreducible construction on compact } g,\end{gathered} \tag{5.9}$$

[15] Broken affine-Sugawara nested graphs are not always new constructions when $N \geqq 3$. For example, breaking all the lines between two lacunae of a complete tripartite graph (coset construction) gives a complete bipartite graph (coset construction)

where c_0 is the high-level central charge of $g^{\#}$. The inequalities (5.9) are true in $SO(n)^{\#}_{\text{diag}}$ as well, since they follow with $c_0 = \dim E$ from the (stronger) *edge theorem*

$$SO(n)^{\#}_{\text{diag}}: n-1 \leqq \dim E(G^{\#}_n(\text{irr})) \leqq \tfrac{1}{2}(n-1)(n-2), \tag{5.10}$$

where $G^{\#}_n(\text{irr})$ is any new irreducible graph of order n. The proof of the edge theorem is as follows: We know from (3.25) that $G^{\#}_n(\text{irr})$ and $\tilde{G}^{\#}_n(\text{irr})$ are both connected, and, moreover, that at least $n-1$ lines are necessary to connect n points. It follows that $c_0 = \dim E(G^{\#}_n(\text{irr}))$ and $\tilde{c}_0 = \dim E(\tilde{G}^{\#}_n(\text{irr}))$ are both greater than or equal to $n-1$. The edge theorem (5.10) follows since $c_0 + \tilde{c}_0 = n(n-1)/2$ on $SO(n)$.

5.5. *Self-K-Conjugate Constructions.* An unlabelled graph G is *self-K-conjugate* (or self-complementary [24]) when $\tilde{G} = G$. At the level of labelled graphs, G and $\tilde{G}$ are isomorphic, and the corresponding constructions $L(G)$ and $L(\tilde{G}) = \tilde{L}(G)$ are $SO(n)$ automorphically equivalent, so that $c = \tilde{c} = c_g/2$ for self-K-conjugate constructions. It follows that a) self-K-conjugate constructions exist only on $SO(4n)$ and $SO(4n+1)$, since $c_0 = \tilde{c}_0 = \dim g/2$ requires that $\dim g$ is even, and b) the *half-Sugawara central charges*

$$\begin{aligned} SO(4n): c &= \frac{xn(4n-1)}{x+4n-2}, \\ SO(4n+1): c &= \frac{xn(4n+1)}{x+4n-1} \end{aligned} \tag{5.11}$$

are determined for self-K-conjugate constructions before obtaining the exact solutions.

The first six self-K-conjugate constructions are given in Fig. 14, and the first three of these were encountered as new irreducible constructions in $SO(4)^{\#}_{\text{diag}}$ and $SO(5)^{\#}_{\text{diag}}$. More generally, the number s_n of self-K-conjugate constructions in $SO(n)^{\#}_{\text{diag}}$

n	4	5	8	9	12	13	16	17
s_n	1	2	10	36	720	5600	703,760	11,220,000

(5.12)

and the asymptotic behavior of s_n

$$\begin{aligned} s_{4n} &= \frac{2^{2n^2-2n}}{n!}(1+\mathcal{O}(n^2/2^{4n})), \\ s_{4n+1} &= \frac{2^{2n^2-n}}{n!}(1+\mathcal{O}(n^2/2^{4n})) \end{aligned} \tag{5.13}$$

are known in graph theory [24].

Although all the self-K-conjugate constructions on a given manifold have the same central charge, each construction is physically distinct (not $SO(n)$ automor-

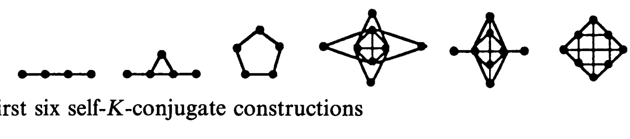

Fig. 14. The first six self-K-conjugate constructions

phically equivalent to any other), with distinct conformal weights, since each construction is a distinct unlabelled graph. Distinct high-level conformal weights on each manifold are easily verified for the graphs of Fig. 14, and are recorded explicitly in Table 3 for the two self-K-conjugate graphs on $SO(5)$.

The exact form of the first three self-K-conjugate constructions is obtained in Sect. 7. The constructions are generically unitary with generically irrational conformal weights, both of which are expected for generic self-K-conjugate constructions. In this circumstance, it is possible to imagine that all the self-K-conjugate solutions in a given $SO(n)_{\mathrm{diag}}$ are connected by a continuous c-fixed quadratic deformation which is a solution of the full master equation on $SO(n)$.

Except in special cases, we have been unable to construct the half-Sugawara central charges (5.11) by affine-Sugawara nesting on any compact g. These central charges, and the values $c=13/10$, $20/11$, and $31/11$ reported on $SU(3)$ [21, 22], should be investigated carefully since the question of new rational central charges is conceptually important.

5.6. Cartesian Product Graphs. Cartesian product graphs [25] may be defined analytically with our original variables $\{\theta_{ij}, \theta_{ii}=0\}$, where $\theta_{ij}=1$ is a line from point i to point j. When $\{\theta_{i_1 j_1}=1\}$ and $\{\theta_{i_2 j_2}=1\}$ are the lines of two graphs G_{n_1} and G_{n_2}, then the Cartesian product graph $G_{n_1 n_2}=G_{n_1}\times G_{n_2}$ is defined on the product points $[i_1, i_2]$ or $[j_1, j_2]$, with lines

$$\theta_{[i_1, i_2];[j_1, j_2]}=\theta_{i_1 j_1}\delta_{i_2 j_2}+\theta_{i_2 j_2}\delta_{i_1 j_1}\,. \tag{5.14}$$

This operation is a direct construction of the high-level inertia tensor $L_{ij}^{(0)}=\theta_{ij}$ of the product graph in terms of the high-level inertia tensors of the component graphs. Pictorially, $G=G_1\times G_2$ is constructed as shown in Fig. 15: Replace each point in (say) G_2 by copies $G_1', G_1'', \ldots$ of the graph G_1, and each line in G_2 by a set of lines which connect only copied points $i', i'', \ldots$ in the copies of G_1. Since the order $n_1 n_2$ of a product graph $G_{n_1 n_2}$ is multiplicative, it is clear that these graphs are a relatively small subset of all graphs.

It is our intuition that

$$\text{conjecture 2: Cartesian product graphs are new constructions} \\ (\text{except } K_2\times K_2 \text{ and } K_1\times G)\,, \tag{5.15}$$

since the product operation is foreign to the affine-Sugawara nesting operations. It suffices to verify conjecture 2 for products $G_1\times G_2$ of two graphs, and in fact only for products of two connected graphs since the identity

$$(G_1\cup G_2)\times G_3=(G_1\times G_3)\cup(G_2\times G_3) \tag{5.16}$$

implies that products of disconnected graphs are new when the products of their connected components are new.

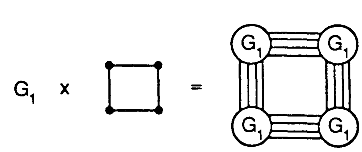

Fig. 15. The Cartesian product graph $G_1\times(K_2\times K_2)$

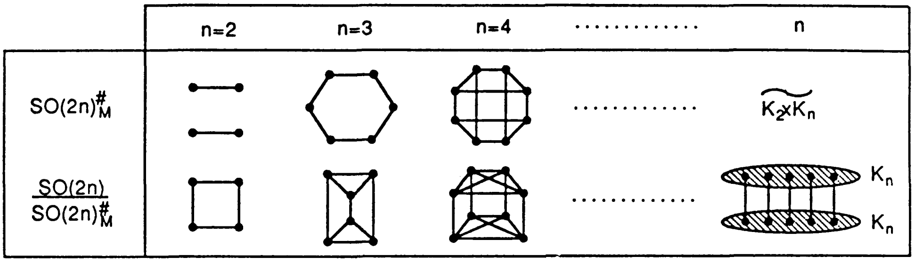

Fig. 16. The maximal-symmetric construction $SO(2n)^{\#}_{M}$

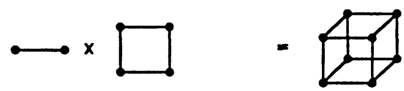

Fig. 17. The n-cubes $Q_n = K_2 \times Q_{n-1}$, $n \geqq 3$ are broken $N=2$ coset graphs and hence new irreducible constructions

With the characterization (3.25) we have checked that conjecture 2 is true for the product graphs through order 8. The conjecture is also true for the maximal-symmetric construction [18]

$$G(SO(2n)/SO(2n)^{\#}_{M}) = K_2 \times K_n \tag{5.17}$$

whose graphs, given in Fig. 16, were identified from the high-level behavior of the known solutions. More generally, the theorem

$$\begin{aligned}&(\text{connected bipartite graph}) \times (\text{connected bipartite graph})\\ &\quad = \text{new irreducible construction (except } K_2 \times K_2) \end{aligned} \tag{5.18}$$

is established pictorially as follows. When G_1 and G_2 are connected graphs with chromatic number two, then $\chi(G_1 \times G_2) = 2$ as well since the two-color scheme of G_1 can be consistently reversed for nearest neighbor copies of G_1 (see Fig. 15). These $\chi = 2$ product graphs are connected and, except for $K_2 \times K_2$, they are incomplete, so (5.18) follows from the theorem in (5.5). $K_2 \times K_2$ is the complete bipartite graph $SO(4)/(SO(2))^2$. An example of this theorem is the set of n-cubes $Q_n \equiv Q_{n-1} \times K_2$, $Q_1 \equiv K_2$ for $n \geqq 3$, shown for $n=3$ in Fig. 17.

6. Graph Symmetry and Consistent Subansätze

In this section, we discuss the *hierarchy of consistent subansätze* in $SO(n)_{\text{diag}}$, which may be determined in principle by studying the symmetry groups auto G_n of the graphs of order n. The subansätze provide the names of the new constructions (see Table 3) and the strategy for exact solutions in the following section.

As a first step, we study the symmetry of the exact solution $L(G)$. Recall from Sect. 3.3 that the lines $\{\theta_{ij} = 1\}$ of G satisfy

$$\theta_{ij} = \theta_{\pi(i)\pi(j)} \tag{6.1}$$

when $\pi\in\operatorname{auto}G$ is a relabelling in the symmetry group of G. The result (6.1) is a high-level symmetry of the construction $L(G)$, expressed as a relation among the high-level components of its inertia tensor $L^{(0)}_{ij}=\theta_{ij}$. In fact, the high-level symmetry (6.1) persists to all orders in the high-level expansion, so that the same symmetry

$$L_{ij}(G)=L_{\pi(i)\pi(j)}(G)\,,\qquad \forall\pi\in\operatorname{auto}G \tag{6.2}$$

is obtained for the exact solution $L(G)$. To see this, one needs the iterative lemma

$$L^{(p)}_{ij}(G)=L^{(p)}_{\pi(i)\pi(j)}(G)\quad\text{when}\quad L^{(q<p)}_{ij}(G)=L^{(q<p)}_{\pi(i)\pi(j)}(G)\,, \tag{6.3}$$

which is not difficult to check from the recursion relation (2.33a). The statement previewed in Sect. 3

$$\text{symmetry group of } L(G)=\text{symmetry group of } G=\operatorname{auto}G \tag{6.4}$$

follows immediately from the result (6.2).

The exact symmetry of $L(G)$ in (6.2) determines the smallest consistent subansatz in which the construction is found. As an exercise, we will determine the smallest subansätze of all the new irreducible constructions in $SO(5)^{\#}_{\text{diag}}$, whose graphs (up to K-conjugation) are given in Fig. 18: The two graphs of Fig. 18a have $\operatorname{auto}G=Z_2$, the non-trivial element being a simultaneous $1\leftrightarrow2$ and $3\leftrightarrow4$ interchange. It follows from (6.2) that both graphs occur first in the six-parameter consistent $SO(5)$ subansatz

$$SO(5)\,[d,6]:L_{12},L_{34},L_{13}=L_{24},L_{14}=L_{23},L_{15}=L_{25},L_{35}=L_{45}\,. \tag{6.5}$$

The two graphs of Fig. 18b occur first in the seven-parameter consistent subansatz

$$SO(5)\,[d,7]:L_{12},L_{34},L_{45},L_{35},L_{13}=L_{23},L_{14}=L_{24},L_{15}=L_{25} \tag{6.6}$$

because $\operatorname{auto}G=Z'_2$ with non-trivial element $\pi=(12)$. Finally, the self-K-conjugate graph of Fig. 18c occurs first in the two-parameter consistent subansatz

$$SO(5)\,[d,2]:L_{12}=L_{13}=L_{24}=L_{35}=L_{45},\;L_{34}=L_{14}=L_{23}=L_{15}=L_{25} \tag{6.7}$$

with $\operatorname{auto}G=D_5$ in this case. The hierarchy of subansätze (6.5–7) is complete for $SO(5)^{\#}_{\text{diag}}$ since each subansatz is K-conjugation covariant.

Note also that $SO(5)\,[d,2]\subset SO(5)\,[d,6]$, so the solutions of $SO(5)\,[d,2]$ will appear as a factorization sector [18, 20, 22] of higher symmetry in the larger subansatz $SO(5)\,[d,6]$. More generally, these factorizations are best studied in sum and difference variables, since, according to (6.2), the appearance of any smaller subansatz is characterized by the vanishing of a set of difference variables $L_{ij}-L_{\pi(i)\pi(j)}$.

We are now in a position to define our labelling scheme for new constructions, which was employed explicitly in Table 3. The general subansatz in $SO(n)_{\text{diag}}$ is

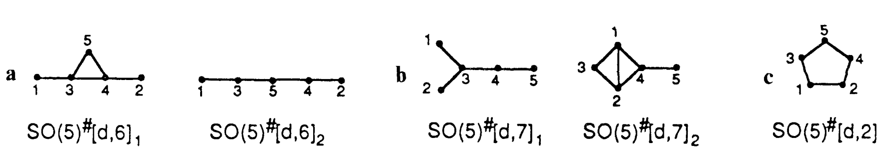

Fig. 18a–c. The labelling is used to obtain the subansatz of the graph

named

$$SO(n)\,[d,s]\,, \tag{6.8}$$

where d denotes the diagonal ansatz and s is the size of the subansatz. For example, Table 3 records that all new irreducible constructions in $SO(6)^{\#}_{\text{diag}}$ are contained in consistent subansätze of size

$$SO(6)^{\#}_{\text{diag}}: s=3,4,5,6,7,7',8,9,9',11, \text{ and } 15\,, \tag{6.9}$$

where $s=15$ is $SO(6)_{\text{diag}}$ itself. Distinct subansätze of the same size are distinguished by primes. The new irreducible solutions are named in their smallest subansatz and numbered according to

$$SO(n)^{\#}\,[d,s]_i\,, \quad i=1,2,\ldots \tag{6.10}$$

when they fall in the lower half of the high-level sectors of the subansatz. This is a complete labelling of solutions in $SO(n)^{\#}_{\text{diag}}$, since the higher sectors are completed by $SO(n)/SO(n)^{\#}\,[d,s]_i$.

An obvious strategy for new exact solutions is to begin with the smaller subansätze, which contain the graphs of higher symmetry. This is a program which we begin in the following section, but which we cannot finish without further insight: The graphs of lower symmetry occur in larger subansätze, and, in particular, the ubiquitous totally-asymmetric identity graphs occur in no subansatz smaller than $SO(n)_{\text{diag}}$ itself.

7. Exact Solutions in $SO(n)^{\#}_{\text{diag}}$

7.1. $SO(2n)^{\#}_{M} \equiv SO(2n)^{\#}\,[d,3]$ *and* $SO(2n)^{\#}\,[d,4]$. The graphs of the maximal-symmetric construction on $SO(2n)$ [18], shown in Fig. 16, are the most symmetric new irreducible graphs in $SO(n)_{\text{diag}}$. The maximal-symmetric construction has auto$\,G = Z_2 \times S_n$ when $n \geqq 3$ (and $Z_2 \times D_4$ at $n=2$) and appears first in the three-parameter subansatz

$$SO(2n)_M \equiv SO(2n)\,[d,3] \begin{cases} L_{ij} = L_{n+i,n+j} = L_h, & 1 \leqq i<j \leqq n \\ L_{i,n+i} = L_c, & 1 \leqq i \leqq n \\ L_{i,n+j} = L_t, & 1 \leqq i \neq j \leqq n \end{cases} \tag{7.1}$$

which is the maximal-symmetric subansatz [18] in Cartesian coordinates [16]. The identification

$$SO(2n)^{\#}_{M} \equiv SO(2n)^{\#}\,[d,3] \tag{7.2}$$

follows for the maximal-symmetric construction in the present taxonomy.

The next most symmetric new irreducible graphs in $SO(2n)_{\text{diag}}$, shown in Fig. 19, have auto$\,G = S_n$, $n \geqq 2$. These constructions appear first in the four-parameter subansatz

$$SO(2n)\,[d,4] \begin{cases} L_{ij} = L_h, \quad L_{n+i,n+j} = L'_h, \quad 1 \leqq i<j \leqq n \\ L_{i,n+i} = L_c, \quad 1 \leqq i \leqq n; \quad L_{i,n+j} = L_t, \quad 1 \leqq i \neq j \leqq n \end{cases} \tag{7.3}$$

[16] The Cartan-Weyl basis of [18] is $\lambda = L_c/(2n-2)$ and $L_{\pm} = (L_t \mp L_h)/2$

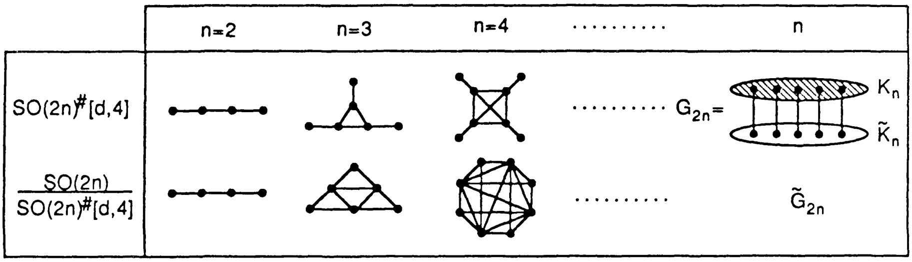

Fig. 19. $SO(2n)^{\#}[d,4]$

which contains the maximal-symmetric subansatz (7.1) when $L_h = L'_h$. In sum and difference variables $L_c^{\pm} \equiv L_c \pm L_t$, $L_h^{\pm} \equiv L_h \pm L'_h$, the explicit form of $SO(2n)[d,4]$ is

$$L_c^-(1-(x+n-2)L_c^+ + (n-2)L_c^- - nL_h^+) = 0\,, \tag{7.4a}$$

$$L_c^+(2-(x+2n-2)L_c^+ + 2(n-2)L_c^-) - (x-2)(L_c^-)^2 - 2(n-2)L_c^- L_h^+ = 0\,, \tag{7.4b}$$

$$L_h^-(1-nL_c^+ + (n-2)L_c^- - (x+n-2)L_h^+) = 0\,, \tag{7.4c}$$

$$\begin{aligned} &L_h^+(2-(x+n-2)L_h^+ + 2(n-2)L_c^- - 2nL_c^+) + (n-4)(L_c^-)^2 \\ &\quad + n(L_c^+)^2 - 2(n-2)L_c^- L_c^+ - (x+n-2)(L_h^-)^2 = 0\,, \end{aligned} \tag{7.4d}$$

$$c = \frac{xn}{2}(nL_c^+ - (n-2)L_c^- + (n-1)L_h^+)\,, \tag{7.4e}$$

which shows the maximal-symmetric subansatz as the factorization sector $L_h^- = 0$ in (7.4c).

The subansatz (7.4) contains 12 known solutions and the following four new solutions:

$$L_c^+ = L_h^+ = \frac{1}{x+2n-2}(1+\eta(n-2)R)\,, \tag{7.5a}$$

$$L_c^- = \eta R\,, \qquad L_h^- = \eta\sigma R\sqrt{\frac{x+n-6}{x+n-2}}\,, \tag{7.5b}$$

$$c = \frac{nx}{2(x+2n-2)}(2n-1-\eta(n-2)(x-1)R)\,, \tag{7.5c}$$

$$R \equiv (x^2+2(n-2)x+n^2-8n+8)^{-1/2}\,, \tag{7.5d}$$

which are labelled by $\eta = \pm 1$, $\sigma = \pm 1$. The values of η correspond to K-conjugation and the values of σ are $SO(2n)$ automorphically equivalent. For either value of σ, these solutions are identified as

$$\begin{aligned} &SO(2n)^{\#}[d,4] : \eta = +1\ (c_0 = n(n+1)/2) \\ &SO(2n)/SO(2n)^{\#}[d,4] : \eta = -1\ (c_0 = 3n(n-1)/2) \end{aligned} \tag{7.6}$$

by matching the high-level form of the central charge in (7.5c) to the number of lines in the graphs of Fig. 19. This family of solutions includes the self-K-conjugate construction [17] $SO(4)^{\#}[d,4]$ and the K-conjugate pair of constructions $SO(6)^{\#}[d,4]$ and $SO(6)/SO(6)^{\#}[d,4]$, all of which appear in Table 3.

[17] The self-K-conjugate construction $SO(4)^{\#}[d,4]$, whose graph is the first in Fig. 19, has the expected central charge $3x/(x+2)$ of $SU(2)$ and irrational conformal weights. Despite the coincidence of central charges, this construction is not a point in the quadratic deformation $(SU(2)\times SU(2))^{\#}$ [18]. $SO(4)^{\#}[d,4]$ should be compared to points in known linear deformations of $SU(2)_x$ [11]

For $x \in \mathbb{N}$, these constructions are unitary down to very low level, as expected: A complete list of nonunitary points is $x=1,2,3$ for $SO(4)$, $x=1,2$ for $SO(6)$ and $x=1$ for $SO(8)$ and $SO(10)$. The constructions are generically irrational, with rational subconstructions only for $n=2$ and levels 1 and 2 of any n [18].

A special point is the level 3 construction $SO(6)_3^{\#}[d,4]$ which is identical to the maximal-symmetric construction $(SO(6)_3^{\#})_M$ at this level. This phenomenon is an isolated equivalence [19] or accidental crossing of solutions at particular finite levels, since the graphs of the constructions are distinct. The value $c(SO(6)_3^{\#}[d,4]) = c((SO(6)_3^{\#})_M) \simeq 2.9597$ is also the lowest unitary irrational central charge in this family of constructions.

7.2. The Subansatz $SO(2n+1)[d,6]$. The most symmetric new irreducible graphs in $SO(2n+1)_{\mathrm{diag}}$, $n \geqq 2$ are the four graph families shown in Fig. 20. All these constructions reside in the six-parameter subansatz

$$SO(2n+1)[d,6]\begin{cases} L_{ij}=L_h, \quad L_{n+i,n+j}=L'_h, \quad 1\leqq i<j\leqq n \\ L_{i,n+i}=L_c, \quad 1\leqq i\leqq n; \quad L_{i,n+j}=L_t, \quad 1\leqq i\neq j\leqq n \\ L_{i,2n+1}=L_r, \quad L_{n+i,2n+1}=L'_r, \quad 1\leqq i\leqq n \end{cases} \tag{7.7}$$

with auto $G=S_n$ when $n\geqq 3$ [20]. The form of $SO(2n+1)[d,6]$ in sum and difference variables is

$$\begin{aligned} &L_c^-(1-(x+n-2)L_c^+ +(n-2)L_c^- -nL_h^+ -L_r^+)=0\,,\\ &L_c^+(2-(x+2n-2)L_c^+ +2(n-2)L_c^- -2L_r^+)-(x-2)(L_c^-)^2\,,\\ &\quad -2(n-2)L_c^- L_h^+ -(L_r^-)^2+(L_r^+)^2=0\,,\\ &L_h^-(1-nL_c^+ +(n-2)L_c^- -(x+n-2)L_h^+ -L_r^+)+L_r^-(L_r^+ -L_h^+)=0\,,\\ &L_h^+(2-(x+n-2)L_h^+ +2(n-2)L_c^- -2nL_c^+ -2L_r^+)+(n-4)(L_c^-)^2\\ &\quad +n(L_c^+)^2-2(n-2)L_c^- L_c^+ -(x+n-2)(L_h^-)^2+(L_r^+)^2+(L_r^-)^2-2L_h^- L_r^- =0\,,\\ &L_r^-(1-nL_c^+ +(n-2)L_c^- -(x+n-1)L_r^+)=0\,,\\ &L_r^+(2-(x+2n-1)L_r^+)-(x-1)(L_r^-)^2=0\,,\\ &c=\frac{xn}{2}(nL_c^+ -(n-2)L_c^- +(n-1)L_h^+ +2L_r^+)\,, \end{aligned} \tag{7.8}$$

where $L_c^\pm$, $L_h^\pm$ are defined in the previous section and $L_r^\pm \equiv L_r \pm L'_r$. This subansatz contains $SO(2n)[d,4]$ when $L_r^- = L_r^+ = 0$, and it also contains the subansatz $SO(5)[d,2]$ when $L_h^+ = L_c^+ = L_r^+$, $L_h^- = L_c^- = -L_r^-$ at $n=2$.

The exact constructions in Sects. 7.3–5 are solutions of the system (7.8). Before the details, here is an overview of the situation.

---

[18] The central charges at levels 1 and 2 are half integer ($\geqq 3/2$) and integer, with irrational conformal weights, so these levels should be compared to particular points of known deformations

[19] Some of these equivalences are well known. For example, the Sugawara construction $SO(2n)_1$ at level 1 is equivalent to the construction on the maximal torus of $SO(2n)$, although the graphs of these constructions are distinct. The equivalence phenomenon also occurs in irrational constructions at rational points which are affine-Sugawara nests

[20] The first column of Fig. 20 shows that the case of $SO(5)$ is special: The graphs at the bottom of the first two graph families are the self-K-conjugate constructions on $SO(5)$, while the third and fourth graph families coincide at order 5. Moreover, the pentagon graph $SO(5)^{\#}[d,2]$ has the higher symmetry auto $G=D_5$, and occurs first in $SO(5)[d,2]$

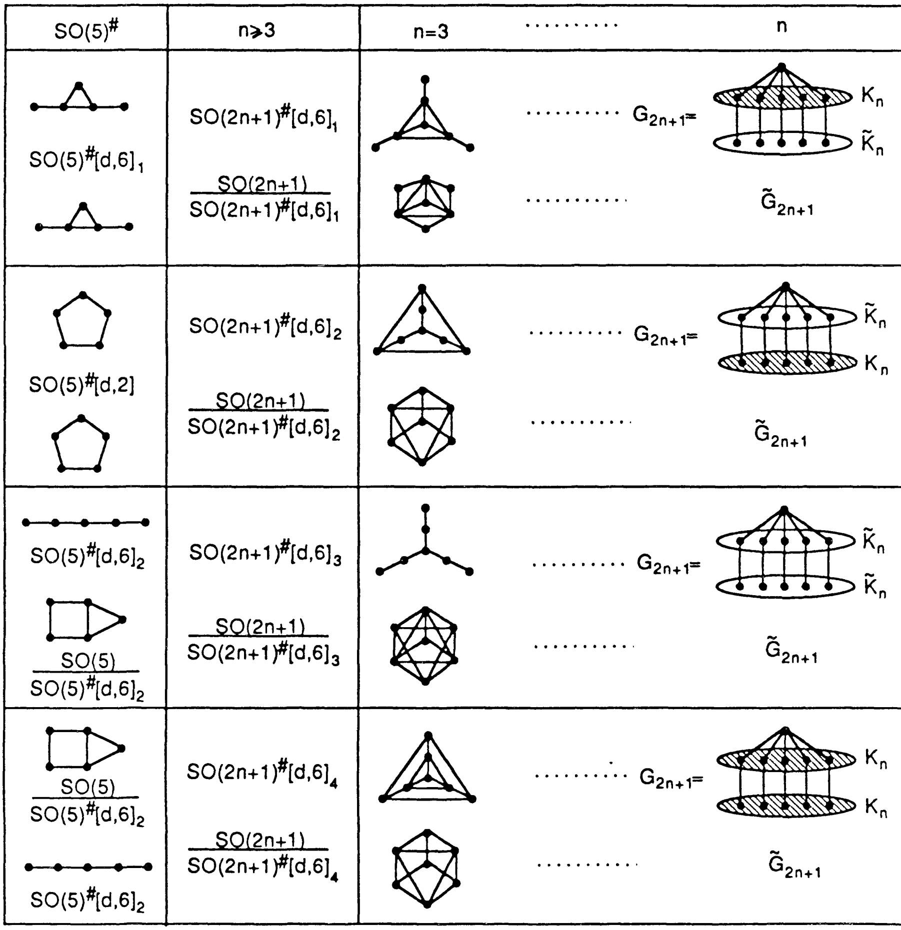

Fig. 20. $SO(2n+1)^{\#}[d,6]$

$SO(2n+1)[d,6]$ contains 48 solutions which are known or were obtained in the previous section, and 64 solutions generically. The generic count of 16 new solutions is accurate except at level 2, where the only new solutions, given in Appendix B, are the new quadratic deformations $SO(2n+1)_2^{\#}[d,6]$ with $c=n$.

Among the 16 new solutions for $x \neq 2$, we will obtain the following 8 solutions across all n,

$$SO(5)^{\#}[d,6]_1 \quad \text{and} \quad SO(5)^{\#}[d,2] \quad (4 \text{ copies each}), \tag{7.9a}$$

$$SO(2n+1)^{\#}[d,6]_{1,2} \quad \text{and} \quad \frac{SO(2n+1)}{SO(2n+1)^{\#}[d,6]_{1,2}} \quad (n \geqq 3,\ 2 \text{ copies each}).$$

These constructions are the first two graph families in Fig. 20. We obtain the remaining 8 solutions only for $n=2$,

$$SO(5)^{\#}[d,6]_2 \quad \text{and} \quad \frac{SO(5)}{SO(5)^{\#}[d,6]_2} \quad (4 \text{ copies each}), \tag{7.10}$$

which are the lowest graphs of the third and fourth graph family in Fig. 20.

7.3. The Self-K-Conjugate Constructions on SO(5). The 8 solutions in Eq. (7.9a) are the self-K-conjugate constructions

$$SO(5)^{\#}[d,6]_1 \begin{cases} L_c^+ = L_h^+ = L_r^+ = \dfrac{1}{x+3}, & x \neq 2 \\ L_c^- = \sigma L_r^- = \dfrac{\sigma x}{x-2} L_h^- = \dfrac{\eta}{\sqrt{(x-1)(x+3)}}, \end{cases} \tag{7.11a}$$

$$SO(5)^{\#}[d,2] \begin{cases} L_c^+ = L_h^+ = L_r^+ = \dfrac{1}{x+3}, & x \neq 2 \\ L_c^- = \sigma L_r^- = -\sigma L_h^- = \dfrac{\eta}{\sqrt{(x-1)(x+3)}}, \end{cases} \tag{7.11b}$$

where $\sigma = \pm 1$ are $SO(5)$ automorphically equivalent and $\eta = \pm 1$ is K-conjugation, which is also an $SO(5)$ automorphism in these cases. Both constructions have the half-Sugawara central charge

$$c = \frac{5x}{x+3}, \quad x \neq 2 \tag{7.12}$$

which is characteristic of self-K-conjugate constructions (see Sect. 5.5).

The self-K-conjugate constructions are unitary for integer $x \geqq 3$. The conformal weights of the vector representation are irrational for $SO(5)^{\#}[d,6]$ and rational for $SO(5)^{\#}[d,2]$, but irrational conformal weights must be expected for higher representations in both cases.

7.4. $SO(2n+1)^{\#}[d,6]_{1,2}$, $n \geqq 3$. The 8 solutions in Eq. (7.9b)[21]

$$L_c^+ = L_h^+ = L_r^+ = \frac{1}{x+2n-1}(1+\eta(n-2)S),$$

$$L_c^- = \eta S, \quad L_h^- = -\eta\sigma \frac{(1-\varepsilon(x+n-3))S}{x+n-2}, \quad L_r^- = \eta\sigma S,$$

$$c = \frac{nx}{2(x+2n-1)}(2n+1-\eta(n-2)(x-2)S), \tag{7.13}$$

$$S \equiv (x^2+2(n-1)x+n^2-6n+5)^{-1/2}, \quad x \neq 2$$

are distinguished by $\eta = \pm 1$, $\sigma = \pm 1$, and $\varepsilon = \pm 1$. The values of η correspond to K-conjugation, the values of σ are $SO(2n+1)$ automorphically equivalent, and the values of ε label physically distinct solutions with the same central charge but different conformal weights.

For $n \geqq 3$, and either value of σ, these solutions are identified as

$$\begin{aligned} &SO(2n+1)^{\#}[d,6]_1 : \varepsilon = \eta = +1 \ (c_0 = n(n+3)/2), \\ &SO(2n+1)/SO(2n+1)^{\#}[d,6]_1 : \varepsilon = -\eta = +1 \ (c_0 = n(3n-1)/2), \\ &SO(2n+1)^{\#}[d,6]_2 : \varepsilon = -\eta = -1 \ (c_0 = n(n+3)/2), \\ &SO(2n+1)/SO(2n+1)^{\#}[d,6]_2 : \varepsilon = \eta = -1 \ (c_0 = n(3n-1)/2). \end{aligned} \tag{7.14}$$

[21] The self-K-conjugate constructions on $SO(5)$ are included in the solutions (7.13) when $n=2$. The identification is $SO(5)^{\#}[d,6]_1$ when $\varepsilon=1$ and $SO(5)^{\#}[d,2]$ when $\varepsilon=-1$

In this case, the identification requires matching $L_{ij}^{(0)}(G)=\theta_{ij}$ for the appropriate graphs against the high level form of the solutions (7.13).

These constructions are unitary for all positive integer level (except $x=2$). They are also generically irrational, with rational subconstructions only at level 1 [22]. The value

$$c((SO(7)_3^{\#})[d,6]_{1,2})=\frac{9}{16}\left(7-\frac{1}{\sqrt{17}}\right)\simeq 3.8011 \tag{7.15}$$

is the lowest unitary irrational central charge in this family.

7.5. $SO(5)^{\#}[d,6]_2$. The 8 solutions on $SO(5)$ in Eq. (7.10)

$$\begin{aligned}
L_c^+ &= \frac{1}{x+3}(1+2\eta(x+1)Q), \quad L_h^+=\frac{1}{x+3}(1-\eta(x+2)(x-1)Q),\\
L_r^+ &= \frac{1}{x+3}(1-4\eta Q), \quad L_c^- = \frac{-\eta\sigma Q}{x-1}\sqrt{(x^2+2)(x^2-4x-2)},\\
L_h^- &= \frac{-L_r^-}{x}=\frac{-\eta\varepsilon Q}{x(x-1)}\sqrt{x(x-4)(x^2+4)},\\
c &= \frac{x}{x+3}(5-\eta(x-1)(x-2)Q),\\
Q &\equiv \sqrt{\frac{x-1}{x^5-x^4-8x^3-4x^2-32x-16}}, \quad x\neq 2
\end{aligned} \tag{7.16}$$

are distinguished by $\eta=\pm1$, $\sigma=\pm1$, and $\varepsilon=\pm1$, where η is K-conjugation, and σ, ε label $SO(5)$ automorphically equivalent solutions. By comparison of graphs and solutions, the identification

$$\begin{aligned}
&SO(5)^{\#}[d,6]_2:\eta=1\ (c_0=4),\\
&SO(5)/SO(5)^{\#}[d,6]_2:\eta=-1\ (c_0=6)
\end{aligned} \tag{7.17}$$

is established for each fixed choice of σ and ε.

These constructions are unitary and irrational for all integer $x\geqq 5$. The value

$$c((SO(5)_5^{\#})[d,6]_2)=\frac{25}{8}\left(1-\frac{4}{5\sqrt{34}}\right)\simeq 2.6963 \tag{7.18}$$

is the lowest unitary central charge of the family, and this value is also the lowest unitary central charge yet observed on non-simply-laced g.

8. The Novelty Number ν

We have constructed a graph function $\nu(G)$ which we call the *novelty number* of G because it appears to distinguish between the graphs $G(AS)$ of the known rational constructions and the graphs $G^{\#}$ of the new constructions,

$$\text{conjecture 3:}\quad \nu(G(AS))=0,\quad \nu(G^{\#})>0. \tag{8.1}$$

[22] The central charges at level one are half integer ($\geqq 3/2$) and integer, with irrational conformal weights, so they should be compared to particular points of known deformations

The novelty number is

$$\nu \equiv -\frac{1}{2}\sum_i d_i(G)(2d_i(G)-1)+9t_3-4t_4+6t_4'-12t_4''+\sum_{(ij)} d_i(G)d_j(G)-2\sum_{(ijk)} d_i(G), \tag{8.2}$$

where

$$t_3 = \text{number of triangles in } G, \quad t_4 = \text{number of squares in } G,$$
$$t_4' = \text{number of squares with one diagonal in } G, \tag{8.3}$$
$$t_4'' = \text{number of } K_4\text{-subgraphs in } G,$$

and the sums in (8.2) are over the lines (ij) of G and the points (ijk) of each triangle in G.

It is sufficient to verify conjecture 3 on connected graphs, since the novelty number is additive $\nu(G_1 \cup G_2) = \nu(G_1) + \nu(G_2)$ on disconnected graphs. The conjecture has been verified for

1. the graphs in the first ten sectors of Table 3,

2. the affine-Sugawara construction K_n and the graphs $\tilde{K}_p + \tilde{K}_{n-p}$ of the fundamental coset constructions $SO(n)/(SO(p) \times SO(n-p))$,

3. the cycle graphs C_{2n} with

$$\nu(C_4)=0; \quad \nu(C_{2n})=2n, \quad n \geqq 3, \tag{8.4}$$

where C_4 is the graph of $SO(4)/(SO(2) \times SO(2))$,

4. the path graphs P_n with

$$\nu(P_2)=0; \quad \nu(P_n)=n-3, \quad n \geqq 3, \tag{8.5}$$

where P_2 and P_3 are the graphs of $SO(2)$ and $SO(3)/SO(2)$,

5. the exact constructions of [18] and Sect. 7 with

$$\begin{aligned}
&\nu(SO(2n)/SO(2n)_M^{\#}) = n(n-1)(n-2),\\
&\nu(SO(2n)^{\#}[d,4]) = n(n-1)/2,\\
&\nu(SO(5)^{\#}[d,2]) = 5,\\
&\nu(SO(5)^{\#}[d,6]_1) = 1,\\
&\nu(SO(2n+1)^{\#}[d,6]_1) = 5n(n-1)/2, \quad n \geqq 3,\\
&\nu(SO(2n+1)^{\#}[d,6]_2) = n(n-1)/2, \quad n \geqq 3,\\
&\nu(SO(5)^{\#}[d,6]_2) = 2.
\end{aligned} \tag{8.6}$$

In cases 3, 4, and 5, we emphasize that the novelty number vanishes precisely for those low n members of the graph family which are affine-Sugawara nested graphs.

Appendix A: Counting Affine-Sugawara Nested Graphs

We first obtain the recursion relation (3.27) for $C(AS)_n$, the number of connected (fundamental) affine-Sugawara nested graphs. The basic idea is to start from the relation

$$C(AS)_n = D(AS)_n \tag{A.1}$$

and express the number of disconnected graphs in terms of $C(AS)_{m<n}$. It is convenient to divide the disconnected graphs into two types I and II,

$$D(AS)_n = D_{\mathrm{I}}(AS)_n + D_{\mathrm{II}}(AS)_n \tag{A.2a}$$

$$D_{\mathrm{I}}(AS)_n \equiv \begin{cases} \text{number of disconnected affine-Sugawara nested graphs} \\ \text{of order } n \text{ with at least one trivial subgraph} \end{cases} \tag{A.2b}$$

$$D_{\mathrm{II}}(AS)_n \equiv \begin{cases} \text{number of disconnected affine-Sugawara nested graphs} \\ \text{of order } n \text{ with no trivial subgraphs} \end{cases} \tag{A.2c}$$

which are counted separately below[23].

I. The disconnected graphs of type I have the form $K_1 \cup$ (general affine-Sugawara nested graph of order $n-1$), so that

$$D_{\mathrm{I}}(AS)_n = 2C(AS)_{n-1} \tag{A.3}$$

follows with Eq. (A.1).

II. The disconnected graphs of type II may be written as

$$\left(\frac{SO(2)}{\vdots}\right)^{p(2)} \times \left(\frac{SO(3)}{\vdots}\right)^{p(3)} \times \ldots \times \left(\frac{SO(n-2)}{\vdots}\right)^{p(n-2)}$$
$$\sum_{i=2}^{n-2} i p(i) = n, \qquad p(i) \geqq 0, \tag{A.4}$$

where the vertical dots indicate arbitrary nesting in each product group $SO(i)$. We emphasize that each of the $p(i)$ factors $(SO(i)/\ldots)$ in the superfactor $(SO(i)/\ldots)^{p(i)}$ is *identical* in unlabelled graph theory.

To count these graphs, we first establish that

$$c(AS)_i^{(p(i))} = \binom{p(i) + c(AS)_i - 1}{p(i)} \tag{A.5}$$

is the number of distinct affine-Sugawara nests in each superfactor $(SO(i)/\ldots)^{p(i)}$, where $C(AS)_i$ is the number of fundamental affine-Sugawara nests in each identical factor $SO(i)$. To understand (A.5), consider first the example of $(SO(3))^3$. There are two fundamental nests $SO(3)$ and $SO(3)/SO(2)$ in each identical $SO(3)$. The distinct nests in $(SO(3))^3$ are

$$\begin{array}{rc|c} & SO(3) & \dfrac{SO(3)}{SO(2)} \\ \hline SO(3) \times SO(3) \times SO(3) = & *** & \\ SO(3) \times SO(3) \times \dfrac{SO(3)}{SO(2)} = & ** & * \\ SO(3) \times \dfrac{SO(3)}{SO(2)} \times \dfrac{SO(3)}{SO(2)} = & * & ** \\ \dfrac{SO(3)}{SO(2)} \times \dfrac{SO(3)}{SO(2)} \times \dfrac{SO(3)}{SO(2)} = & & *** \end{array}, \tag{A.6}$$

[23] Examples of type I on $SO(6)$ are $SO(5) \times SO(1) = SO(5)$ and $SO(5)/(SO(4) \times SO(1)) = SO(5)/SO(4)$, while $SO(2) \times SO(4)$ is type II because it uses all six points

where the right-hand side phrases the example as the placement of $p(i)=3$ identical objects $*$ in $C(AS)_i=2$ boxes. The result is $C(AS)_i^{(3)}=\binom{3+2-1}{3}=4$ distinct nests in the superfactor $(SO(3))^3$.

More generally, $C(AS)_i^{(p(i))}$ is computable as the number of ways to place $p(i)$ identical objects in $C(AS)_i$ boxes, which is also the number of ways to partition $p(i)$ identical objects with $C(AS)_i-1$ walls (the dotted line in Eq. (A.6)). Equivalently, the result (A.5) is the number of ways to place $p(i)$ identical objects on a total number $p(i)+C(AS)_i-1$ of available sites = objects plus walls.

The total number of nests at fixed $\{p(i)\}$ is a product over the nests of each superfactor, and the result for type II nests

$$D_{\mathrm{II}}(AS)_n=\sum_{\{p(i)\}}\prod_{\substack{i=2\\p(i)\neq 0}}^{n-2}\binom{p(i)+C(AS)_i-1}{p(i)} \tag{A.7}$$

is obtained by summing over all partitions $\{p(i)\}$.

Having computed $D_{\mathrm{I}}(AS)_n$ and $D_{\mathrm{II}}(AS)_n$ in terms of $C(AS)_{m<n}$, the recursion relation for $C(AS)_n$, given in Eq. (3.27) of the text, follows with Eqs. (A.1), (A.2), (A.3), and (A.7).

We remark in passing that the same argument on the set of *all* disconnected graphs gives the following relation:

$$\begin{aligned}C_n&=g_n-D_n=g_n-(D_{\mathrm{I},n}+D_{\mathrm{II},n})\\&=g_n-g_{n-1}-\sum_{\{p(i)\}}\prod_{\substack{i=2\\p(i)\neq 0}}^{n-2}\binom{p(i)+C_i-1}{p(i)}\end{aligned} \tag{A.8}$$

which may be used to compute C_n from $C_{m<n}$ and g_n. C_n is computed from g_n by a different route in [24].

We finally establish an upper bound on $C(AS)_n$ as follows. Any disconnected graph of order $n=$ odd may be decomposed as

$$(\text{connected graph of order } 1\leqq i\leqq(n-1)/2)\cup(\text{graph of order } n-i) \tag{A.9a}$$

for one or more values of i. Similarly, any disconnected graph of even order may be decomposed either as

$$(\text{connected graph of order } 1\leqq i\leqq(n-2)/2)\cup(\text{graph of order } n-i) \tag{A.9b}$$

for one or more values of i, or as

$$(\text{connected graph of order } n/2)\cup(\text{connected graph of order } n/2). \tag{A.9c}$$

Then, the upper bound on all disconnected graphs

$$D_n\leqq\begin{cases}\displaystyle\sum_{i=1}^{(n-1)/2}C_i g_{n-i} & n=\text{odd}\\ \displaystyle\sum_{i=1}^{(n-2)/2}C_i g_{n-i}+(C_{n/2})^2 & n=\text{even}\end{cases} \tag{A.10}$$

follows because the decompositions (A.9) are not unique.

The bound (A.10) may be restricted to affine-Sugawara nested graphs, so that the simple upper bound

$$C(AS)_n=D(AS)_n\leqq\sum_{i=1}^{n-1}C(AS)_i C(AS)_{n-i} \tag{A.11}$$

is obtained with $D(AS)_n = C(AS)_n$, $g(AS)_{n-i} = 2C(AS)_{n-i}$ and symmetry about $i = n/2$. The right-hand side of (A.11) is an upper bound on the right-hand side of the recursion relation (3.27) for $C(AS)_n$, so the solution $C(AS)_n^{(\max)}$ of the simple recursion relation

$$C(AS)_n^{(\max)} = \sum_{i=1}^{n-1} C(AS)_i^{(\max)} C(AS)_{n-i}^{(\max)}, \qquad C(AS)_1^{(\max)} = 1 \tag{A.12}$$

satisfies $C(AS)_n \leqq C(AS)_n^{(\max)}$. The solution of (A.12) is

$$C(AS)_n^{(\max)} = \frac{1}{2(2n-1)} \binom{2n}{n}, \qquad C(AS)_n \leqq \frac{1}{2(2n-1)} \binom{2n}{n} \tag{A.13}$$

which implies the asymptotic bound in Eq. (3.29b) of the text.

Appendix B: The Deformations $SO(2n+1)_2^{\#}[d,6]$, $n \geqq 2$

The only new solutions at level 2 of $SO(2n+1)[d,6]$ are the two-parameter quadratic deformations which we call $SO(2n+1)_2^{\#}[d,6]$,

$$\begin{gathered} L_c^+ = \frac{1}{n}(1-(n+1)L_r^+ + (n-2)L_c^-), \qquad L_h^+ = L_r^+, \\ L_r^- = \eta R, \qquad L_h^- = \frac{\eta}{n}[-R + \varepsilon\sqrt{1-4(L_c^-)^2}], \\ R \equiv \sqrt{L_r^+(2-(2n+1)L_r^+)}, \\ c = n. \end{gathered} \tag{B.1}$$

The deformations are labelled by $\varepsilon = \pm 1$, $\eta = \pm 1$ and arbitrary values of the deformation parameters L_r^+ and L_c^-. The values of ε label two distinct deformations within the construction. The unitary range of the deformation parameters

$$0 \leqq L_r^+ \leqq \frac{2}{2n+1}, \qquad -\frac{1}{2} \leqq L_c^- \leqq \frac{1}{2} \tag{B.2}$$

defines a rectangle in parameter space. At fixed ε, the construction is closed under K-conjugation on $SO(2n+1)$

$$\tilde{L}_\eta^{\#}(L_r^+, L_c^-) = L_{-\eta}^{\#}\left(\frac{2}{2n+1} - L_r^+, -L_c^-\right) \tag{B.3}$$

which shows that K-conjugation in this case is $\eta \to -\eta$ plus a reflection about the center of the unitary rectangle.

The conformal weights of $SO(2n+1)_2^{\#}[d,6]$ are continuous functions of the deformation parameters, and we have checked that the construction is not equivalent to any known quadratic deformation. The physical content of the construction should, as usual, be compared to known linear deformations [11].

Acknowledgements. We wish to thank O. Alvarez, I. Bakas, M. Crescimanno, S. Hotes, E. Kiritsis, D. Smit, and E. Wichmann for helpful conversations.

References

1. Kač, V.G.: Simple graded Lie algebras of finite growth. Funct. Anal. App. **1**, 328–329 (1967)
Moody, R.V.: Lie algebras associated with general Cartan matrices. Bull. Am. Math. Soc. **73**, 217–221 (1967)
2. Bardakci, K., Halpern, M.B.: New dual quark models. Phys. Rev. D **3**, 2493–2506 (1971)
3. Ramond, P.: Dual theory for free fermions. Phys. Rev. D **3**, 2415–2418 (1971)
4. Halpern, M.B.: The two faces of a dual pion-quark model. Phys. Rev. D **4**, 2398–2401 (1971)
5. Halpern, M.B.: Quantum "solitons" which are $SU(N)$ fermions. Phys. Rev. D **12**, 1684–1699 (1975)
6. Banks, T., Horn, D., Neuberger, H.: Bosonization of the $SU(N)$ Thirring models. Nucl. Phys. B **108**, 119–129 (1976)
7. Frenkel, I.B., Kač, V.G.: Basic representations of affine Lie algebras and dual resonance models. Inv. Math. **62**, 23–66 (1980)
Segal, G.: Unitary representations of some infinite dimensional groups. Commun. Math. Phys. **80**, 301–342 (1981)
8. Witten, E.: Non-abelian bosonization in two dimensions. Commun. Math. Phys. **92**, 455–472 (1984)
Segal, G.: unpublished
Knizhnik, V.G., Zamolodchikov, A.M.: Current algebra and Wess-Zumino model in two dimensions. Nucl. Phys. B **247**, 83–103 (1984)
9. Goddard, P., Kent, A., Olive, D.: Virasoro algebras and coset space models. Phys. Lett. **152** B, 88–92 (1985)
10. Gross, D., Harvey, J.A., Martinec, E., Rohm, R.: Heterotic string. Phys. Rev. Lett. **54**, 502–505 (1985)
11. Freericks, J.K., Halpern, M.B.: Conformal deformation by the currents of affine g. Ann. Phys. **188**, 258–306 (1988); Erratum, ibid. **190**, 212 (1989)
12. Halpern, M.B.: Direct approach to operator conformal constructions: From fermions to primary fields. Ann. Phys. **194**, 247–280 (1989)
13. Goddard, P., Olive, D.: Kac-Moody and Virasoro algebras in relation to quantum physics. Int. J. Mod. Phys. A **1**, 303–414 (1986)
14. Frenkel, I.B., Lepowsky, J., Meurman, A.: To appear
15. Halpern, M.B., Kiritsis, E.: General Virasoro construction on affine g. Mod. Phys. Lett. A **4**, 1373–1380 (1989); Erratum ibid. A **4**, 1797 (1989)
16. Halpern, M.B., Yamron, J.P.: Geometry of the general affine-Virasoro construction. Nucl. Phys. B **332**, 411–424 (1990)
17. Morozov, A.Yu., Perelomov, A.M., Rosly, A.A., Shifman, M.A., Turbiner, A.V.: Quasi-exactly-solvable quantal problems: One-dimensional analogue of rational conformal field theories. Int. J. Mod. Phys. A **5**, 803–832 (1990)
18. Halpern, M.B., Kiritsis, E., Obers, N.A., Porrati, M., Yamron, J.P.: New unitary affine-Virasoro constructions. Int. J. Mod. Phys. A **5**, 2275–2296 (1990)
19. Witten, E.: The central charge in three dimensions. Memorial Volume for V. Knizhnik, Brink, L. et al. (eds.). World Scientific: Singapore 1990
20. Halpern, M.B., Obers, N.A.: Unitary irrational central charge on compact g. I. (simply-laced $g_x)_{\#}^{q \geqq 2}$. Int. J. Mod. Phys. A **6**, 1835–1857 (1991)
21. Schrans, S., Troost, W.: Generalized Virasoro constructions for $SU(3)$. Nucl. Phys. B **345**, 584–606 (1990)
22. Halpern, M.B., Obers, N.A.: Unitary irrational central charge on compact g. II. High-level analysis and $SU(3)^{\#}_{\mathrm{BASIC}}$. Nucl. Phys. B **345**, 607–644 (1990)
23. Halpern, M.B., Yamron, J.P.: A generic affine-Virasoro action. Nucl. Phys. B **351**, 333–352 (1991)
24. Harary, F., Palmer, E.M.: Graphical enumeration. New York, London: Academic Press 1973
25. White, A.T.: Graphs, groups and surfaces. Amsterdam, London: North-Holland/American Elsevier 1973

Communicated by N. Yu. Reshetikhin